A serum-free media formulation for cultured meat production supports bovine satellite cell differentiation in the absence of serum starvation

ARTICLES
https://doi.org/10.1038/s43016-021-00419-1
nature food

A serum-free media formulation for cultured meat production supports bovine satellite cell differentiation in the absence of serum starvation

Tobias Messmer[1,2], Iva Klevernic[1], Carolina Furquim[1], Ekaterina Ovchinnikova[1], Arin Dogan[1], Helder Cruz[1], Mark J. Post[1,2] and Joshua E. Flack[1]✉

Cultured meat production requires the robust differentiation of satellite cells into mature muscle fibres without the use of animal-derived components. Current protocols induce myogenic differentiation in vitro through serum starvation, that is, an abrupt reduction in serum concentration. Here we used RNA sequencing to investigate the transcriptomic remodelling of bovine satellite cells during myogenic differentiation induced by serum starvation. We characterized canonical myogenic gene expression, and identified surface receptors upregulated during the early phase of differentiation, including *IGF1R*, *TFRC* and *LPAR1*. Supplementation of ligands to these receptors enabled the formulation of a chemically defined media that induced differentiation in the absence of serum starvation and/or transgene expression. Serum-free myogenic differentiation was of similar extent to that induced by serum starvation, as evaluated by transcriptome analysis, protein expression and the presence of a functional contractile apparatus. Moreover, the serum-free differentiation media supported the fabrication of three-dimensional bioartificial muscle constructs, demonstrating its suitability for cultured beef production.

'Cultured' or 'cultivated' meat is an emerging technology based on the proliferation and differentiation of stem cells in vitro to produce edible tissues for human consumption. Its development is motivated primarily by sustainability issues associated with traditional meat production, including greenhouse gas emissions, resource consumption, animal welfare and food safety[1,2].

Cultured meat is composed primarily of skeletal muscle tissue, which can be grown from adult stem cells known as muscle satellite cells (SCs) and from several other cell types[3,4]. Previous work has described the isolation and proliferation of SCs from skeletal muscle, and their myogenic differentiation in hydrogels or scaffolds to form three-dimensional (3D) bioartificial muscles (BAMs) through the use of tissue engineering techniques[5,6].

However, to become commercially viable, cultured meat technologies must overcome a critical dependence on animal-derived components[2]. Standard protocols for SC proliferation require fetal bovine serum (FBS) at concentrations of up to 20%, which affords efficient growth rates, and enables myogenic differentiation through an abrupt reduction in serum concentration, a process referred to as 'serum starvation'[7]. Scientific concerns (including batch-to-batch variation), cost, and ethical and consumer acceptance anxieties necessitate the replacement of FBS-supplemented culture media with chemically defined, animal-free alternatives for cultured meat production in the absence of transgene expression. Although chemically defined media have now been developed that support the differentiation of muscle cell lines such as C2C12, induced pluripotent stem cells (iPSCs), embryonic stem cells (ESCs) and SCs all rely on serum starvation and/or transgene overexpression to induce differentiation[8–11].

Differentiation of SCs into mature muscle fibres requires extensive transcriptional remodelling, including the downregulation of cell-cycle-related genes, upregulation of myogenic transcription factors and membrane fusogens, and the production of a functional contractile apparatus upon terminal differentiation[12,13]. Activation of master transcriptional regulators occurs early in this process, but the mechanisms whereby serum starvation induces these changes remain poorly understood[7,14]. Whereas previous studies have focused on myogenesis during embryonic development in cattle and other species[15–18], the transcriptional landscape of adult bovine myogenic differentiation in vitro has not been studied in a detailed chronological fashion.

In this article we use bulk mRNA sequencing (RNA-seq) to study gene expression profiles during muscle differentiation upon serum starvation. By supplementing agonists to upregulated surface receptors, we develop a chemically defined medium that can drive robust myogenic differentiation in the absence of serum starvation and/or transgene expression.

Results

Serum starvation triggers widespread transcriptomic change. We induced myogenic differentiation of bovine satellite cells through withdrawal of serum (from 20% in growth medium (GM), to 2% in differentiation medium (DM); hereinafter referred to as 'serum starvation'), and studied the resulting transcriptomic and proteomic profiles (Fig. 1a,b). After 96 h, the fusion index (the percentage of nuclei within multinucleated myotubes[19]) increased from 1.0% to 38.3% (Fig. 1c), whilst nuclei counts did not show a specific trend (Fig. 1d). Performing principal component analysis (based on the 500 most variably expressed genes), samples clustered by time point, independent of batch, indicating that the day of differentiation explained the majority of the variation (Fig. 1e). The greater Euclidean distance between 0 and 48 h, compared to that between 48 and 96 h, suggests that the majority of transcriptional remodelling occurs within the first two days.

We used the RNA-seq dataset to assess gene expression of prominent myogenic transcription factors and canonical differentiation

[1]Mosa Meat BV, Maastricht, the Netherlands. [2]Department of Physiology, Maastricht University, Maastricht, the Netherlands. ✉e-mail: joshua@mosameat.com

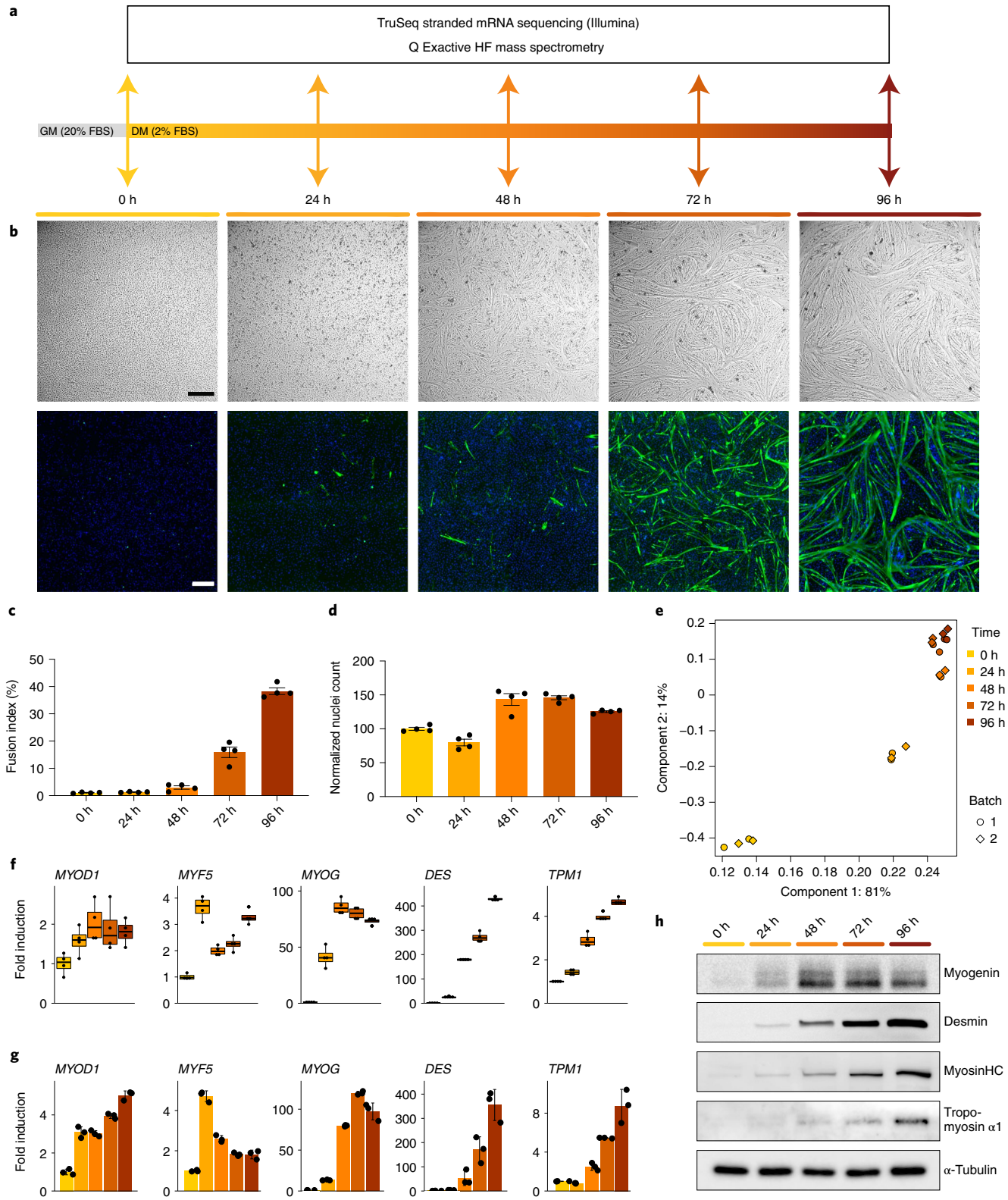

Fig. 1 | Bovine SCs undergo extensive transcriptomic changes upon serum starvation. a, Experimental design for the transcriptomic and proteomic characterization of differentiating bovine SCs at 0 h, 24 h, 48 h, 72 h and 96 h following serum starvation. **b**, Representative bright-field (top row) and fluorescence (bottom row) images corresponding to time points in **a**. Green, desmin; blue, Hoechst. Scale bars, 500 μm. **c**, Mean quantified fusion indices of images in **b**. Error bars indicate s.d. **d**, Normalized nuclei count of **b** as a percentage of mean count at 0 h. Error bars indicate s.d. **e**, Principal component analysis of the 500 most variably expressed genes in differentiating SCs from 0 to 96 h. Colours indicate the time after serum starvation. **f**, Median fold expression changes of muscle-related genes compared to 0 h as determined by RNA-seq during the time course of serum starvation. Boxes indicate interquartile range (IQR); whiskers show 1.5 × IQR. **g**, Mean fold expression changes of genes shown in **f**, determined by RT–qPCR. Error bars indicate s.d., $n = 4$. **h**, Muscle-related protein expression during time course of serum starvation, as measured by western blot.

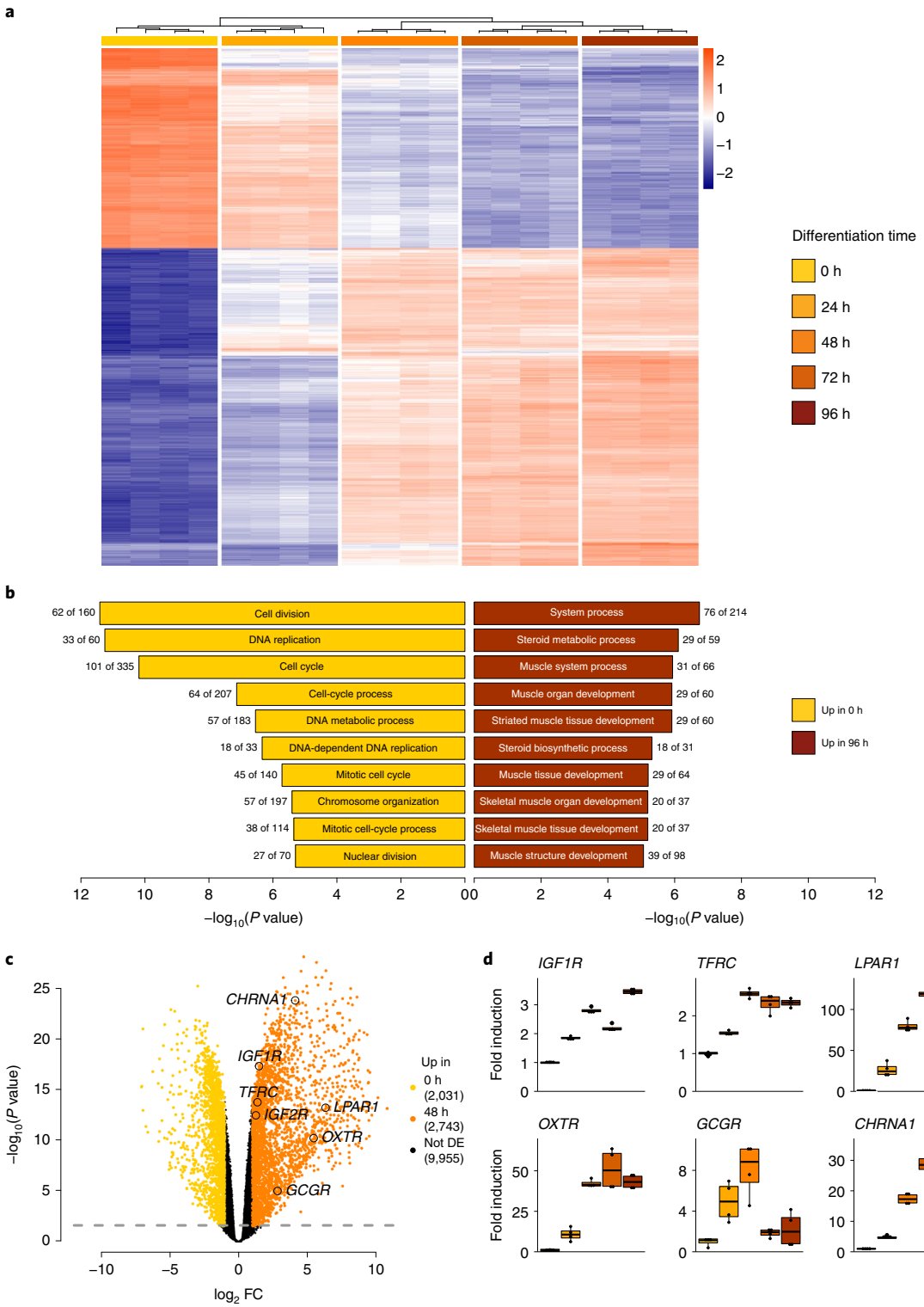

Fig. 2 | Differential expression analysis identifies surface receptors upregulated upon serum starvation. a, Heatmap showing *z* values of the 1,000 most differentially expressed genes between 0 and 96 h after serum starvation. Genes (rows) and samples (columns) were clustered via Ward's method and *z* values bounded at −2.5 and 2.5. Colours above samples indicate time after serum starvation. **b**, Bar plot indicating gene ontology terms (biological processes) corresponding to genes differentially expressed between 0 h (yellow) and 96 h (red). Proportion of significantly up/downregulated genes of total genes per gene ontology term is indicated. **c**, Volcano plot showing differentially expressed genes between 0 h (yellow) and 48 h (orange). Genes corresponding to selected differentially expressed surface receptors are highlighted; dashed line indicates *P* value at FDR = 0.05. DE, differentially expressed. **d**, Median fold changes from 0 to 96 h post serum starvation, normalized against 0 h, for selected significantly upregulated surface receptors, determined via RNA-seq. Boxes indicate IQR; whiskers show 1.5 × IQR.

markers, and found them to be consistently upregulated over the course of differentiation (Fig. 1f and Extended Data Fig. 1a)[20,21]. Myogenic regulator *MYF5* was most highly expressed 24 h following serum starvation, while expression of stem cell marker *PAX7* increased during the first 24 h, before being downregulated (as previously shown in mouse[22]). Expression patterns of these genes were confirmed via quantitative real-time polymerase chain reaction (RT–qPCR) (Fig. 1g and Extended Data Fig. 1b), and by assessing protein levels via western blot (Fig. 1h). Moreover, we also observed increased expression of skeletal-muscle-specific myosins[23] and myoblast fusogens[13] over time, while expression of satellite cell markers, cell-adhesion-related and cell-cycle-maintenance genes decreased concomitantly (Extended Data Fig. 1c,d).

Surface receptors upregulated upon serum starvation. We performed differential expression analysis to identify genes up- and downregulated during differentiation (Fig. 2a). In total, 2,984 of 14,729 genes were significantly upregulated between 0 and 96 h ($\log_2$FC > 1, FDR < 0.05, where FC is fold-change and FDR is false discovery rate), while 2,438 were significantly downregulated ($\log_2$FC < −1, FDR < 0.05; Extended Data Fig. 2a). Upregulated genes between 0 and 96 h predominantly encode proteins related to muscle development and function, protein folding, cell-cycle inhibitors and cadherins (Supplementary Table 1). Gene ontology terms associated with these genes relate to muscle processes or muscle development (upregulation) and to cell-cycle regulation (downregulation; Fig. 2b), suggesting that serum starvation induces differentiation through cell-cycle arrest, as previously described[7,24]. We noted that transcriptional remodelling upon serum starvation is largely conserved between bovine and mouse ($R = 0.65$; Extended Data Fig. 2b) when comparing the gene expression changes between 0 and 96 h with those previously observed between 0 and 120 h for C2C12 cells[25].

We subsequently compared observed changes in gene expression with changes in protein levels. Our mass spectrometry analysis identified 719 proteins for which the corresponding gene was present in the RNA-seq dataset. We determined significantly up- and downregulated proteins over the course of differentiation (Supplementary Table 2), which included muscle-specific markers such as desmin, myosin heavy chain (myosinHC) and tropomyosin-α1. These proteins showed similar expression profiles to those previously observed via western blot (Extended Data Fig. 2c and Fig. 1h). We then compared the $\log_2$FC in protein levels identified via mass spectrometry with $\log_2$ FC in gene expression quantified by RNA-seq, between the earliest and the latest time points of differentiation analysed. The strong correlation ($R = 0.78$; Extended Data Fig. 2d) observed implies that transcriptomic changes during myogenic differentiation generally translate into corresponding changes in protein levels.

Reasoning that activation of cell-surface receptors upregulated during early differentiation might promote initiation of myogenic differentiation in vitro in the absence of serum starvation, we identified genes encoding surface receptors that were upregulated between 0 and 48 h ($\log_2$ FC > 1, FDR < 0.05). Amongst these were *IGF1R* and *IGF2R*, encoding receptors mediating signalling of insulin, IGF1 and IGF2 (ref. [26]), and the genes for transferrin (*TFRC*), lysophosphatidic acid (LPA; *LPAR1*), oxytocin (*OXTR*), glucagon (*GCGR*) and acetylcholine (*CHRNA1*) receptors (Fig. 2c,d). We confirmed upregulation of each of these receptors during differentiation by RT–qPCR (Extended Data Fig. 2e).

Ligands of upregulated receptors induce differentiation. To induce differentiation in the absence of serum starvation, we supplied activatory ligands to the surface receptors previously identified as upregulated during the early phase of differentiation, and investigated the effect on myogenic differentiation (Fig. 3). We initially supplemented basal DMEM/F-12 with $NaHCO_3$, L-ascorbic acid 2-phosphate, EGF1, MEM amino acids and serum albumin based on serum-free media formulations for iPSCs and SCs[27,28]. This formulation (hereinafter referred to as serum-free base (SFB)) increased nuclei count by 76% relative to DMEM/F-12, indicating increased cell survival, but did not significantly increase the fusion index (Fig. 3a,b).

As transferrin receptor (TfR1) and IGF1R were amongst the most significantly upregulated surface receptors (and because ligands for these are widely used components of culture media[26]), we next supplemented SFB with transferrin and insulin. Supplementation with transferrin (T, 135 nM) alone did not have a significant effect on fusion index, whereas insulin (I, 1.8 μM) increased fusion from 7.4% (s.d. = 1.8) to 12.3% (s.d. = 1.3; $P < 0.001$, $n = 4$; Fig. 3c). A synergistic effect was observed upon addition of both components, resulting in an increased fusion index of 30.8% (s.d. = 1.8; $P < 0.001$, $n = 4$), although still less than the 39.0% (s.d. = 0.7) observed in serum starvation.

To approach the extent of differentiation induced by serum starvation, we then supplemented transferrin- and insulin-containing SFB with additional ligands to other upregulated receptors, in varying concentrations (Fig. 3d,e). The fusion index increased significantly from 30.7% (s.d. = 2.6) to 38.1% (s.d. = 2.0; $P = 0.022$, $n = 4$) and 41.0% (s.d. = 2.7; $P < 0.001$, $n = 4$) upon addition of 1 and 10 μM LPA, respectively, and to 38.2% (s.d. = 2.6; $P = 0.019$, $n = 4$) on addition of 1 μM glucagon, whereas the effect of oxytocin or ACh supplementation was not statistically significant (Fig. 3f).

Serum-free differentiation mimics serum starvation. Supplementation of SFB with transferrin, insulin and LPA (a formulation hereinafter referred to as serum-free differentiation medium (SFDM)) resulted in fusion indices comparable to those of serum starvation controls. We characterized the extent of differentiation induced by SFDM more thoroughly, by assessing gene expression of canonical myogenic markers (Fig. 4a). *MYOD1*, *MYOG*, *DES* and *TPM1* showed significantly greater induction (between 0 and 72 h) for both SFDM and serum starvation conditions when compared to SFB. The same trend was observed for protein expression levels (Fig. 4b), indicating that SFDM induces a myogenic phenotype similar to serum starvation. For some genes (*MYOG* and *DES*) and proteins (for example, myosinHC), induction in SFDM was lower than in serum starvation.

To confirm that serum-free differentiation was not dependent on surface coating, we tested SFB, SFDM and serum starvation on a selection of extracellular matrix protein coatings (Fig. 4c). Compared with Matrigel, there was no significant difference in fusion index on any coating, with the exception of Laminin-111. Nuclei count and myotube morphology were variable throughout the conditions, although similar trends were observed for serum starvation controls (Fig. 4d and Extended Data Fig. 3a). We next studied the performance of SFDM and serum starvation with respect to fusion index as a function of number of population doublings (PDs) prior to differentiation. At early passage, serum starvation controls performed slightly better than SFDM, but at higher PDs, SFDM and serum starvation showed similar fusion index (Fig. 4e and Extended Data Fig. 3b,c), indicating that SFDM might show improved performance in aged cells. We also compared the extent and variability of myogenic differentiation across SCs from additional donor animals, and found that fusion indices in SFDM were largely comparable to serum starvation (although for several donor animals, serum starvation did show a minor but statistically significant increase; Extended Data Fig. 4).

During longer time courses (up to ten days) of differentiation, we occasionally observed spontaneous contraction of myotubes. We therefore studied functional differentiation by performing electrical pulse stimulation (EPS) after 192 h of serum-free differentiation[29].

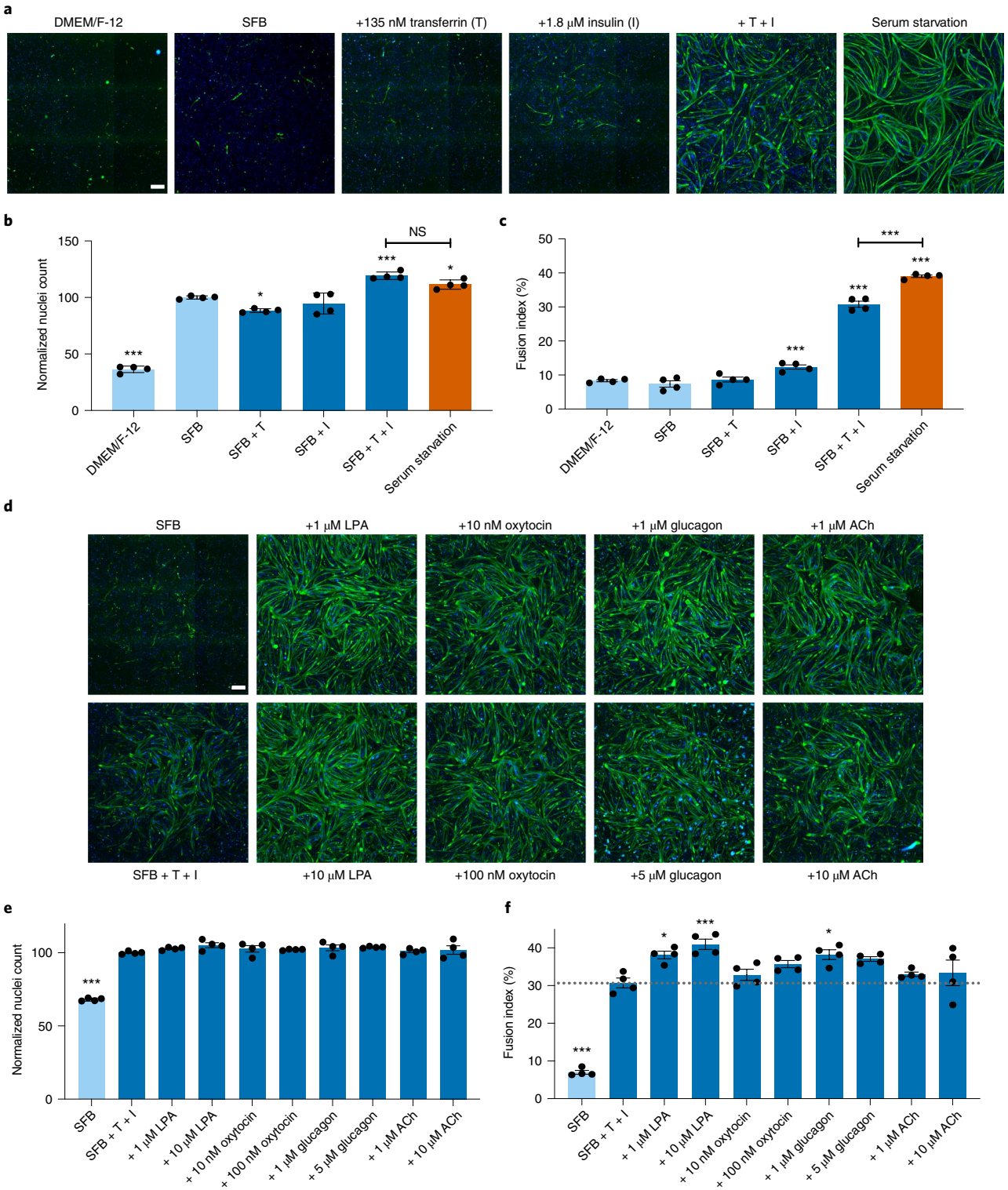

Fig. 3 | Serum-free differentiation is induced by supplementation of ligands to upregulated receptors. a, Representative fluorescence images of SCs after 72 h in SFB media with (blue) and without (light blue) supplementation of insulin (I, 1.8 μM), transferrin (T, 135 nM) and both, with basal DMEM/F-12 and serum starvation as reference controls. Green, desmin; blue, Hoechst. Scale bar, 500 μm. **b**, Nuclei counts derived from images in **a** and three additional replicates as percentage against SFB media. Error bars indicate s.d., $n = 4$. NS, not significant. **c**, Mean fusion indices derived from images in **a** and three additional replicates, calculated by the percentage of nuclei within desmin-positive areas of total nuclei. Statistical significance is indicated for each condition against SFB, as well as between SFB + T + I and serum starvation. Error bars indicate s.d., $n = 4$. **d**, Representative fluorescence images of SCs after 72 h in SFB + T + I with additional supplementation of LPA, oxytocin, glucagon and acetylcholine (ACh). Green, desmin; blue, Hoechst. Scale bar, 500 μm. **e**, Nuclei counts derived from images in **d** and three additional replicates as a percentage of SFB + T + I. Statistical significance is indicated for each condition against SFB + T + I, error bars indicate s.d., $n = 4$. **f**, Mean fusion indices derived from images in **d** and three additional replicates. Statistical significance is indicated for each condition against SFB + T + I; grey line indicates SFB + T + I baseline; error bars indicate s.d., $n = 4$. $^{*}P < 0.05$, $^{**}P < 0.005$, $^{***}P < 0.001$.

EPS at 0.5 and 1 Hz resulted in rhythmic myotube contractions, indicating formation of a functional contractile apparatus sensitive to membrane depolarization (Fig. 4f and Supplementary Video 1). Tetanic contraction was observed upon EPS at 5 Hz, or upon addition of 100 µM ACh.

Transcriptomic profiling of serum-free differentiation. Given that our serum-free conditions induced myogenic differentiation to a similar extent to serum starvation, we next characterized and compared the underlying transcriptional changes in depth, by performing RNA-seq prior to and after 72 h of treatment with SFB, SFDM, and serum starvation (Fig. 5). Dimensionality reduction showed that samples were most clearly separated between 0 h (GM, SFGM) and 72 h (SFB, SFDM, DM; Fig. 5a), suggesting that the three 72 h time points share an extensive set of differentially regulated genes.

To assess the overall similarity of gene expression changes, we determined differentially expressed genes during serum-free and serum-starvation-induced differentiation, and compared the respective $\log_2$FC values between 0 and 72 h (Fig. 5b). Although slightly more genes were significantly up- and downregulated during serum starvation, the strong correlation observed ($R = 0.73$) suggests that the general transcriptomic changes induced are very similar, indicating that the same underlying biological mechanisms are being activated. To examine this trend more specifically, we interrogated the dataset for expression of certain myogenic regulators and muscle markers (Fig. 5c). Induction of expression of *MYOD1*, *MYOG* and *DES* was similar during serum-free and serum-starvation-induced differentiation, while SFB also led to a small increase in expression of these genes, as previously observed (Fig. 4a). However, genes associated with late-stage differentiation, such as *MYH2*, showed significantly higher expression in serum starvation, indicating that terminal differentiation may be more pronounced after 72 h of serum starvation than the same period of serum-free differentiation. Indeed, the increased Euclidean distance between DM and the undifferentiated samples, relative to that for SFDM (Fig. 5a), suggests that serum starvation triggers myogenic gene expression programs in a faster or more pronounced fashion than serum-free differentiation.

SFDM supports cultivation of differentiated BAMs. Most concepts for production of cultured meat require the cultivation of 3D muscle constructs. We therefore assessed the potential of SFDM for promoting the formation and maturation of myotubes during the fabrication of BAMs. We embedded differentiating SCs in collagen/Matrigel hydrogels for 192 h in serum-free differentiation and serum starvation conditions (Fig. 6a), and assessed the structure and differentiation of the resulting BAMs via confocal microscopy, western blot and scanning electron microscopy (SEM).

During pilot studies, we noted that different basal media appeared to affect the overall morphology of BAM constructs. We confirmed that the supplements present in SFDM result in pronounced 2D myogenic differentiation in both DMEM/F-12 and DMEM basal media (Extended Data Fig. 5). Neither nuclei number nor fusion index differed significantly between DMEM/F-12- and DMEM-based serum-free differentiation (Extended Data Fig. 6b,c). In addition, we observed a strong correlation in transcriptional changes induced in DMEM/F-12- and DMEM-based SFDM as measured by RNA-seq ($R = 0.83$, Extended Data Fig. 5d). We thus tested both formulations in BAM fabrication.

All conditions resulted in the formation of viable constructs after eight days of culture (Extended Data Fig. 6a). Cell density and alignment, as well as actin and myosin expression, were visibly more pronounced in SFDM and DM when compared to SFB (Fig. 6b), suggesting a more differentiated myogenic phenotype. Furthermore, we identified desmin expression exclusively in DMEM-based SFDM and serum starvation control BAMs, which was increased further by addition of ACh after 96 h (Extended Data Fig. 6b). The presence of large myotubes at the surface of constructs (Fig. 6c and Extended Data Fig. 6c) suggests that DMEM-based SFDM supplemented with ACh was the best serum-free media formulation, supporting myotube formation in BAMs comparable to serum starvation. Protein expression of canonical muscle differentiation markers was strongly induced (and to a similar extent) in both DMEM/F-12- and DMEM-based serum-free BAMs, although to a lesser extent than in serum starvation (Fig. 6d).

Discussion

Production of cultured meat requires robust differentiation of stem cells into mature muscle fibres, without the use of serum or other animal-derived components. Chemically defined media have previously been developed that support the myogenic differentiation of primary SCs from mouse[8,30], human[9] and other species[31], and for cell lines, iPSCs[26] and ESCs[10]. However, these protocols invariably rely on use of serum during the proliferation phase to induce differentiation through serum starvation, and/or on transgenic overexpression of transcription factors such as MyoD[11,32]. We aimed to solve this issue by developing a chemically defined medium that can drive robust differentiation in the absence of both serum starvation and transgene expression.

We characterized with high resolution the transcriptomic and proteomic changes that occur during differentiation of bovine satellite cells upon serum starvation. Changes in mRNA expression observed during myogenic differentiation correlated well with changes in protein levels. In addition, they exhibited similar patterns to those previously found in cattle and other species[17,25,33], indicating that transcriptional remodelling processes occurring during muscle differentiation are well conserved. Interestingly, switching from SFGM to a minimal medium formulation (SFB) induced transcriptional changes that somewhat resembled serum starvation, suggesting that withdrawal of growth factors and other components partially reproduces the effects of serum starvation, and that reduction in the activity of pro-mitotic signalling pathways (such as those stimulated by FGF2) contributes to induction of differentiation. Additionally, our transcriptomic analysis identified several cell-surface receptors upregulated during the early phase of differentiation. By supplementing the minimal medium with ligands to

Fig. 4 | Serum-free differentiation is of comparable extent to serum starvation. a, Mean gene expression fold changes for SFB (light blue), SFDM (blue) and serum starvation (orange) 72 h after induction of differentiation, normalized to respective conditions at 0 h (not shown), as determined by RT-qPCR. Error bars indicate s.d., $n = 3$. **b**, Muscle-related protein expression after 0 and 72 h in SFB, SFDM and serum control, as measured by western blot. **c**, Representative fluorescence images of differentiating SCs after 72 h in SFDM on indicated coatings. Green, desmin; blue, Hoechst. Scale bar, 500 µm. **d**, Fusion index corresponding to **c** with SFB and serum starvation control. Significance was determined for each condition separately against the respective Matrigel control. Error bars indicate s.d., $n = 3$. **e**, Fusion indices after 72 h in SFB, SFDM or upon serum starvation of SCs corresponding to early (left), medium (centre) and late (right) passages with indicated population doublings. Significance was determined against SFB and between SFDM and serum starvation for each time point. Error bars indicate s.d., $n = 4$. **f**, Relative size change of a myotube during EPS over time with varying frequencies, and on addition of H_2O or ACh. Each point represents a measurement of relative distance of two fixed points from Supplementary Video 1; dashed lines delineate indicated parameter changes. $^*P < 0.05$, $^{**}P < 0.005$, $^{***}P < 0.001$.

these receptors, we developed a chemically defined medium that afforded robust myogenic differentiation in 2D and 3D assays, and which induced transcriptional and phenotypic changes with strong similarities to serum starvation.

Several of the pathways we stimulated have been related to myogenic differentiation. Insulin and transferrin have previously been identified as myotrophic factors both individually and synergistically[34–36]. These effects have been linked to increased glucose uptake

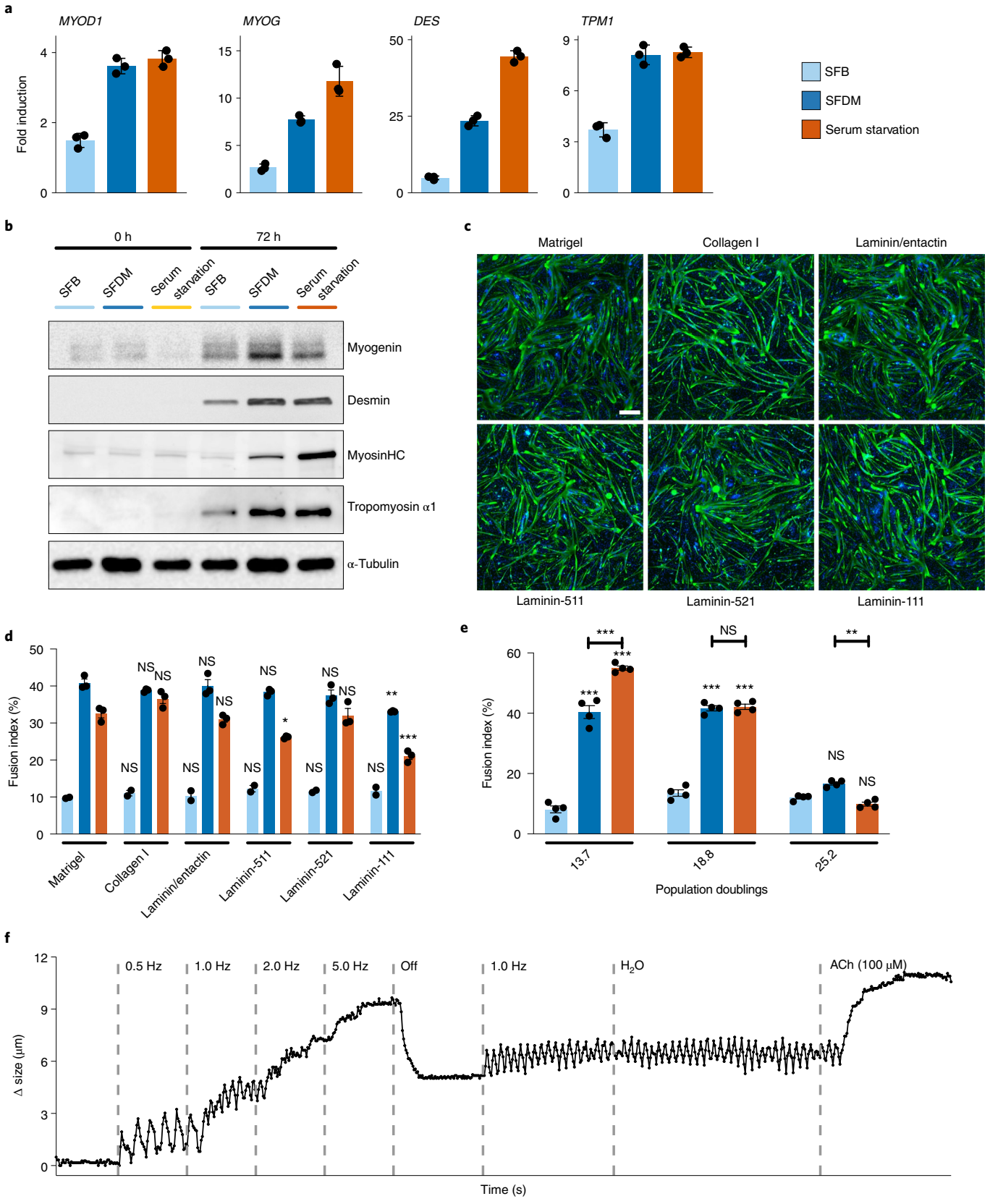

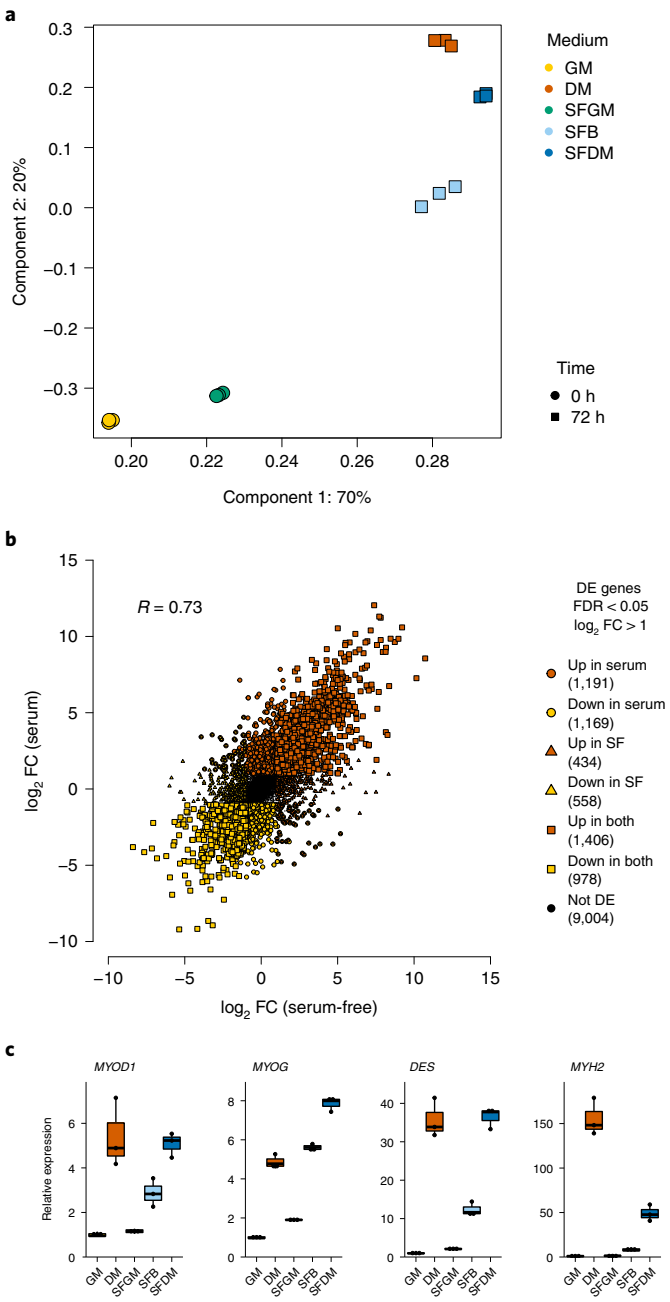

Fig. 5 | Transcriptional remodelling during serum-free differentiation is similar to serum starvation. a, RNA-seq-derived principal component analysis of the 500 most variably expressed genes before and after switching from GM (0 h) and SFGM (0 h) to serum starvation (DM) or SFB/SFDM, respectively, for 72 h. **b**, Scatter plot of $\log_2$ FC between SFGM and SFDM (*x* axis) versus those between GM and DM (*y* axis) with Pearson correlation coefficient (*R*) as indicated. Data points represent genes differentially expressed as indicated, with respective counts shown. **c**, Median fold expression changes for selected genes upon serum starvation and serum-free differentiation, each normalized to GM, determined via RNA-seq. Boxes indicate IQR; whiskers show 1.5 × IQR.

and improved iron homeostasis, although no clear mechanism of action connecting both pathways has been described[34,35]. We also found that activation of the glucagon receptor, a class B GPCR, had a mild pro-myogenic effect, despite previous observations that it is not expressed at high levels in skeletal muscle in vivo[37,38]. Taken together, these data suggest a complex role for the insulin and glucagon signalling pathways, probably linked to glucose metabolism in vitro, and offer a potential avenue to further improve our SFDM formulation through the tuning of glucose levels and other metabolites. Use of metabolomic approaches to assess stabilities and consumption rates of other medium components, such as amino acids, will enable further optimization of feeding strategies during myogenic differentiation.

LPAR1-mediated signalling has been reported to facilitate migration of activated SCs, through stimulation of the sphingosine kinase and sphingosine 1-phosphate pathways[39]. Interestingly, we observed that LPA supplementation at concentrations up to 10 µM yielded a pro-myogenic effect, whereas previous studies have linked higher concentrations to inhibition of differentiation in C2C12 cells[40]. Conversely, neither oxytocin nor ACh significantly affected differentiation in our 2D differentiation assays, despite indications from past studies to the contrary[27,41]. However, supplementation of SFDM with ACh did promote formation of myotubes in BAMs, suggesting that myotube detachment from 2D surfaces may conceal the effects of ligands which promote the later stages of differentiation[42]. Addition of such 'maturation factors' could help promote expression of terminal differentiation-related genes, such as *MYH2*, which were not induced as strongly in SFDM.

Our SFDM formulation supports the myogenic differentiation of 3D muscle organoids in the absence of serum starvation and/or transgene expression. Various animal-free models have previously been proposed for the fabrication of cultured meat, including plant-based scaffolds and polymeric hydrogels[43,44]. While the hydrogels used in this study were not fully animal-component free, we observed robust 2D differentiation on several recombinant extracellular matrix components, and we expect that these findings will be reproduced in fully animal-free organoid cultures. Further modifications are likely to positively impact the extent of differentiation achieved in 3D, and to reduce costs. Refining the composition and directionality of extracellular matrix proteins can enhance SC motility and alignment, leading to more pronounced myofibril development[45]. Similarly, EPS of muscle organoids has been shown to improve force generation, leading to increased expression of myoglobin and other mature muscle markers[29,46]. Finally, expanding the 3D model to include co-culture with other cell types, such as endothelial cells or fibroblasts, could promote myogenic differentiation through juxtacrine or paracrine interactions[6,9]. In this way, increased tissue complexity might narrow the disparity between current cultured meat models and traditional meat.

Other scientific challenges remain crucial hurdles to widespread success of cultured meat technologies. Significant proliferation is required to produce substantial amounts of cultured meat from a small number of starting cells[47]. Although serum-free differentiation outperformed serum starvation at high PDs, neither showed evidence of substantial myotube formation. This is probably attributable to a loss of SC stemness independent of differentiation conditions, and can be addressed by mitigating cellular aging effects using small molecules or growth factors to inhibit specific signalling pathways (such as p38/MAPK)[48]. Furthermore, cultured meat production will require reproducibility over a broad range of donor animals, breeds and (ideally) species. We tested SCs from eight Belgian Blue cattle, all of which demonstrated myogenic differentiation, but to a variable extent when compared to serum starvation. Further research is needed to clarify and mitigate sources of donor-to-donor variability. Nevertheless, the development of culture conditions that permit myogenic differentiation in the absence of serum starvation and transgene expression is an important step towards the realization of cultured meat.

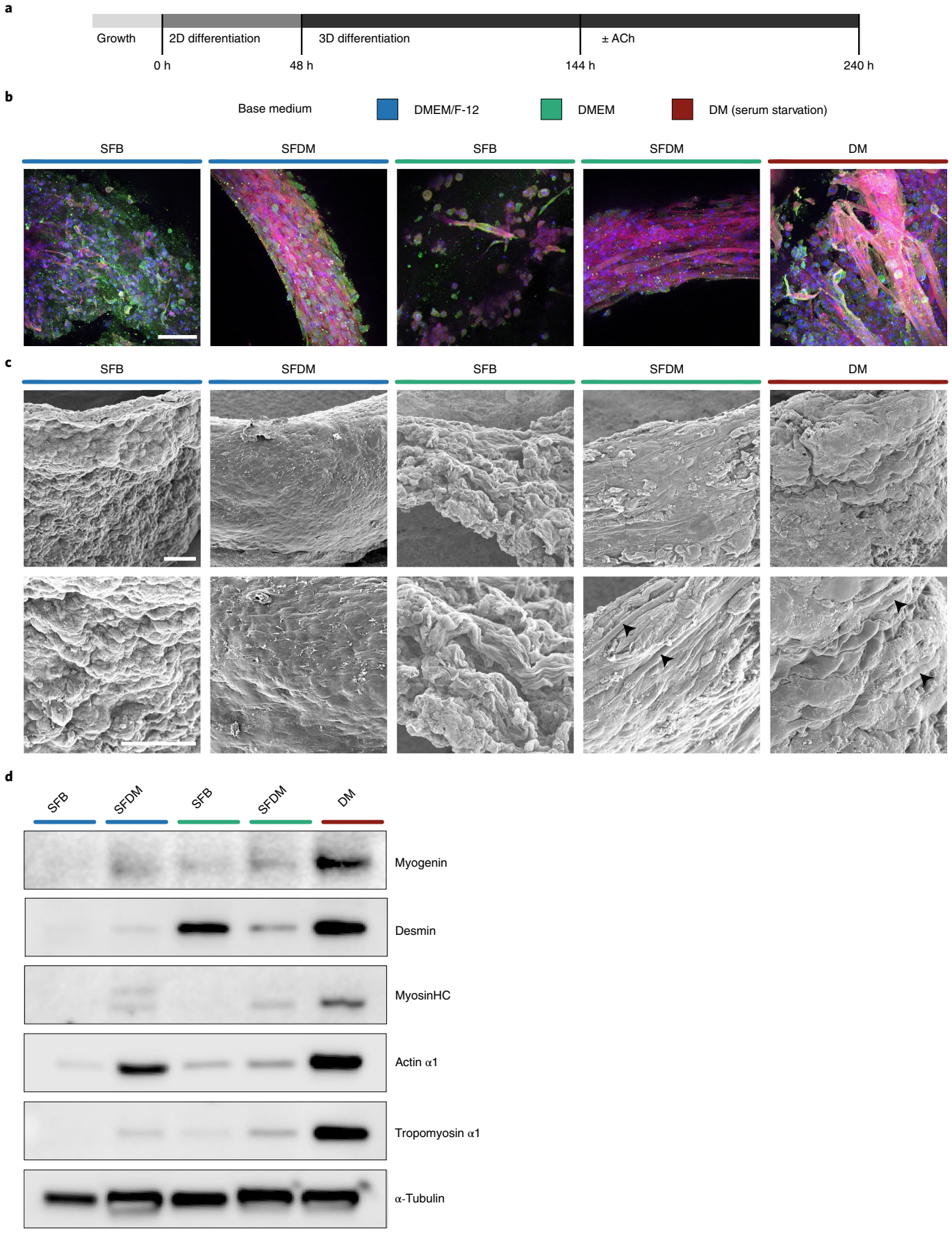
a
Growth
2D differentiation
3D differentiation
± ACh
0 h
48 h
144 h
240 h
b
Base medium
DMEM/F-12
DMEM
DM (serum starvation)
SFB
SFDM
SFB
SFDM
DM
c
SFB
SFDM
SFB
SFDM
DM
d
SFB
SFDM
SFB
SFDM
DM
Myogenin
Desmin
MyosinHC
Actin α1
Tropomyosin α1
α-Tubulin

Fig. 6 | Serum-free differentiation medium enables fabrication of bioartificial muscles. a, Experimental setup for BAM fabrication in collagen/Matrigel hydrogels. **b**, Maximum intensity projection confocal microscopy images of BAMs after 192 h in SFB and SFDM (DMEM/F-12 and DMEM based) or DM. Pink, desmin, red, α-actin; green, myosinHC; blue, Hoechst. Scale bar, 100 µm. **c**, Wide (top) and close-up (bottom) SEM images of BAMs after 192 h in SFB and SFDM (DMEM/F-12 and DMEM based) or DM. Arrowheads indicate myotube formation. Scale bars, 100 µm. **d**, Canonical muscle protein expression in BAMs after 192 h in SFB, SFDM or upon serum starvation, as measured by western blot.

Methods

Satellite cell isolation and culture. Bovine SCs were isolated and purified as previously described[48]. Briefly, freshly obtained semitendinosus muscle from slaughtered Belgian Blue cattle (both male and female, aged from 1 to 7 yr) was minced and then digested with collagenase (CLSAFA, Worthington) for 1 h at 37 °C before filtration with 100 µm nylon cell strainers. Red blood cells were lysed with ammonium–chloride–potassium lysis buffer, filtered with 40 µm strainers and cultured for 72 h in SFGM. SCs were purified by fluorescence-activated cell sorting on a FACSAria Fusion Cell Sorter (BD Biosciences). Cells were stained with NCAM1-PE-Cy7 (335826, BD Biosciences), CD29-APC (B247653, BioLegend), CD31-FITC (MCA1097F, Bio-Rad) and CD45-FITC (MCA2220F, Bio-Rad) and SCs sorted by gating for the CD31/CD45–, CD29+/NCAM1+ population.

SCs were cultured on flasks coated with Collagen Type I solution (Collagen from Bovine Skin, Merck) in either GM or SFGM (Extended Data Table 1). Cells were passaged every 4–5 days upon approaching confluency.

Myogenic differentiation. SCs were differentiated on 0.5% Matrigel-coated plates (except where noted) by seeding 5×10^4 cells cm^{-2} in either GM (for serum starvation) or SFGM (for serum-free differentiation). Differentiation was induced by changing to DM after 24 h (for serum starvation), or by exchanging SFGM for serum-free differentiation medium (SFDM) or the media composition as indicated.

Immunofluorescent staining. Cells were fixed with 4% PFA, permeabilized with 0.5% Triton X-100 and blocked in 5% bovine serum albumin (BSA). Fixed cells were stained with α-desmin antibody (D1033, Sigma-Aldrich) and Hoechst 33342 (Thermo Fisher Scientific), and imaged using an ImageXpress Pico Automated Cell Imaging System (Molecular Devices).

Nuclei counts were determined by quantifying Hoechst staining using MetaXPress software, and normalized against respective controls. The fusion index was determined by quantifying nuclei within desmin-stained myofibres as a proportion of total nuclei and multiplying by 100 (refs. [33,34]).

RT–qPCR. Cell lysates were harvested by adding TRK lysis buffer (Omega Bio-tek) to tissue culture samples after removing culture media and washing with PBS. RNA was purified using the Omega MicroElute Total RNA Kit (Omega Bio-tek). RNA concentrations were determined by spectrophotometry and reverse-transcribed using the iScript cDNA synthesis kit (Bio-Rad). RT–qPCR was performed using iQ SYBR Green Supermix (Bio-Rad) with primer pairs shown in Extended Data Table 2. The resulting cycle threshold (CT) values were averaged across three technical replicates, ΔCTs were calculated and the $2^{\Delta CT}$ of genes of interest were normalized against 'housekeeping' genes (*B2M* and *RPL19*). Statistical significance between respective fold changes was evaluated using Dunnett's multiple-comparison test against respective controls.

RNA sequencing. *Library preparation and sequencing.* Sequencing libraries were prepared from harvested RNA samples using the TruSeq stranded mRNA kit (Illumina) and sequenced on a high-output 75 bp NextSeq 500 (Illumina). For GSE173198 (Fig. 1) and GSE173196 (Fig. 5), 37.0×10^6 (s.d. = 7.3×10^6) and 31.0×10^6 (s.d. = 3.6×10^6) aligned reads were obtained per sample on average, respectively.

Read alignment and quantification. STAR aligner v.2.7 was used to align single-end reads to the reference genome bosTau9 (ARS UCD1.2.98). Subsequent analysis was performed in R v.4.1.0. Gene counts based on the aligned reads were quantified using the FeatureCounts function of the Rsubread package[49]. For GSE173198, 78.86% (s.d. = 1.04) and for GSE173196, 80.39% (s.d. = 1.77) of reads were uniquely assigned to genes.

Quality control and normalization. DGEList-object was created using the obtained count matrix and gene meta information from the Btaurus_gene_ensembl dataset[50]. Low-abundance genes (below a count of 10 for every individual sample, below a minimum count of 15 when summed over all samples, or not expressed in at least two replicates for every condition) were removed, and normalization factors were calculated using the trimmed-mean of M-values method in the NormFactor function of edgeR[51]. Counts per million (CPM) and reads-per-kilobase per million (RPKM) were computed based on normalized library sizes.

Dimensionality reduction and differential expression analysis. Principal component analyses were performed using the 500 most variable genes based on the variance of RPKMs. Differential expression analysis was performed for each gene between all conditions using the limma package according to its suggested workflow at default parameters, that is, by transforming the counts into $\log_2$CPM values, estimating mean variance and computing observation-based weights (voom function), fitting a linear model (lmFit function), computing estimated coefficients (contrasts.fit function) and performing empirical eBayes moderation (eBayes function) towards a common value with a $\log_2$FC threshold of 1.2 (ref. [52]). Genes were considered differentially expressed above a $\log_2$FC cutoff of 1 and an FDR < 0.05, and were visualized in volcano plots. A heatmap showing the *z* values of the 1,000 most differentially expressed genes between 0 and 96 h was constructed in which genes and samples were clustered using Ward's minimum variance method with Euclidean distances. Overrepresented gene ontology terms were computed for both upregulated and downregulated genes[53].

Western blotting. Cells were lysed on ice using the RIPA Lysis Buffer System (Santa Cruz Biotechnology). Protein samples were boiled in Laemmli buffer for 5 min, separated by SDS–PAGE on 4–20% Mini-Protean TGX Gels (Bio-Rad), and transferred to PVDF membranes by electroblotting. Membranes were stained with primary antibodies against desmin (D1033, Sigma-Aldrich), myogenin (sc-52903, Santa Cruz Biotechnology), tropomyosin-α1 (ab133292, Abcam), myosinHC β (M8421, Sigma-Aldrich), α-actin (ab97373, Abcam) and α-tubulin (ab4074, Abcam) and respective secondary antibodies α-mouse-horseradish peroxidase (ab6721, Abcam) and α-rabbit-horseradish peroxidase (P0447, Dako). Protein bands were detected with SuperSignal West Femto Maximum Sensitivity Substrate (Thermo Fisher Scientific) and visualized on an Azure 600 chemiluminescence imager (Azure Biosystems).

Mass spectrometry. *Sample preparation.* Protein samples were collected as triplicates in 5 M urea, 50 mM ammonium bicarbonate and lysed by three freeze–thaw cycles. Samples were reduced with 20 mM dithiothreitol and alkylated with 40 mM iodoacetamide. Alkylation was terminated by addition of 30 mM dithiothreitol to consume excess iodoacetamide. Digestion was performed for 2 h at 37 °C in a thermoshaker (Grant Instruments) with Lys-C/trypsin mix (Promega, V5073), which was added at a ratio of 1:25 (enzyme to protein). Lysates were diluted with 50 mM ABC to 1 M urea for overnight digestion, which was terminated by addition of formic acid to a total of 1%.

Liquid chromatography. Peptide separation was performed on a Dionex Ultimate 3000 Rapid Separation UHPLC system (Thermo Fisher Scientific), equipped with a PepSep C18 analytical column (length, 15 cm; inner diameter, 75 µm; 1.9 µm Reprosil; 120 Å). Peptide samples were first desalted on an online installed C18 trapping column. After desalting, peptides were separated on the analytical column with a 90 min linear gradient from 5% to 35% acetonitrile with 0.1% FA at 300 nl min^{-1} flow rate. The UHPLC system was coupled to a Q Exactive HF mass spectrometer (Thermo Fisher Scientific). Data-dependent acquisition settings were as follows: full MS scan between *m*/*z* 250 and 1,250 at a resolution of 120,000 followed by MS/MS scans of the top 15 most intense ions at a resolution of 15,000.

Mass spectrometric raw data analysis. For protein identification and quantitation, data-dependent acquisition spectra were analysed with MaxQuant (Max Planck Institute). The Andromeda search engine was used with the SwissProt Bovine database (SwissProt TaxID, 9913). Dynamic modifications of methionine oxidation and protein N-terminus acetylation and static modification of cysteine carbamidomethylation were taken into account.

Quality control and data processing. Data were processed and analysed using the DEP package in R (ref. [54]). First, a summarized-experiment object was created based on label-free quantitation (LFQ) intensities from the MaxQuant output. A total of 1,169 proteins were identified after filtering for proteins that were present in all replicates of at least one condition; there were an average of 659.8 (s.d. = 84.3) proteins per sample and 381 proteins present in all samples. Data were normalized by variance stabilization transformation resulting in log LFQ intensities before imputation by assuming missing-not-at-random values and using the MiniProb method.

Differential expression analysis and Pearson correlation. Differential protein expression between samples was determined through log LFQ intensities using empirical eBayes moderation. The most significantly differentially enriched proteins between 0 and 72 h were computed (FDR < 0.05, $\log_2$FC > 1) and a Pearson correlation coefficient was calculated against the transcriptional $\log_2$FCs between 0 and 96 h.

EPS. Cells were differentiated as previously described in SFDM for 192 h in six-well plates. EPS was applied to cells using a C-PACE EP stimulator (IonOptix) with six-well electrodes at 12.0 V and 1.0 ms pulse width. Contraction of myotubes was recorded at 60 f.p.s. with an Evos FL5000 microscope (Thermo Fisher Scientific). Size changes were quantified by measuring pixel distance between two fixed points on the myotubes in every fifth frame of Supplementary Video 1 using ImageJ. Sizes were converted to nanometres (using the microscope scale bar for reference) and plotted against time.

BAM fabrication. Cells were cultured for one passage in either SFGM or GM on Matrigel-coated flasks until they reached confluence. Differentiation was induced by switching from SFGM to SFB or SFDM as indicated, or from GM to DM. After 48 h in SFB, SFDM or DM, cells were harvested and filtered with a 70 µm nylon strainer. BAMs were fabricated by modifying a previously described method[5]. Briefly, 5.9×10^6 cells ml^{-1} in respective media were mixed with 1.5 mg ml^{-1} ice-cold Collagen Type I solution (Merck) and neutralized with 0.5 N NaOH (Sigma) solution by mixing on ice. Matrigel (Corning) was mixed within the gel to a final percentage of 7%, and 70 µl plated around a stainless steel pillar (2 mm in diameter). After allowing the hydrogel to compact for 2 h, respective differentiation media were added. Media changes were performed after 96 h (ACh was included in the medium at a final concentration of 10 µM where indicated) and BAMs were harvested a total of 192 h after fabrication.

Confocal microscopy. BAMs were washed in ice-cold PBS, fixed in 4% PFA and harvested by careful removal from pillars. Fixed structures were stained with primary antibodies against desmin (D1033, Sigma-Aldrich) and myosinHC (M8421, Sigma-Aldrich) and subsequently with secondary antibodies α-rabbit-Alexa488 (A21206,Thermo Fisher Scientific) and α-mouse-Alexa633 (A21050, Thermo Fisher Scientific), and with Phalloidin-490LS (14479, Sigma-Aldrich) and Hoechst 33342 (Thermo Fisher Scientific). Images of stained BAM constructs were captured using a TCS SP8 MP confocal microscope (Leica Microsystems), and are presented as single slices or maximum-intensity projections as indicated.

SEM. BAM constructs were transferred to Karnovsky fixative at room temperature (2% PFA, 2.5% glutaraldehyde in 0.1 M NaH_2PO_4, C0250, Sigma-Aldrich). BAMs were washed in 0.1 M NaH_2PO_4 and postfixed for 1 h with 1% OsO_4, 1.5% ferrocyanide in 0.1 M cacodylate. After postfixative was removed, BAMs were washed, dehydrated by critical point drying and sputter-coated with a thin gold layer using a SC7620 Mini Sputter Coater (Quorum Technologies). The prepared samples were imaged on a JSM-IT200 InTouchScope scanning electron microscope (JEOL).

Statistical analyses. Statistical significance for nuclei counts and fusion indices was assessed using Prism v.9.1.2 (GraphPad). In the case of one dependent variable, one-way analysis of variance was performed to determine statistical significance, followed by Dunnett's multiple-comparison test against indicated controls (Fig. 3 and Extended Data Fig. 5). In the case of two independent variables, two-way analysis of variance was performed, followed by Tukey's multiple-comparison test (Fig. 4 and Extended Data Figs. 3 and 4). Sample replicates consisted of cells from the same donor animal, cultured in separate vessels. No statistical methods were used to predetermine sample sizes, but sample sizes are similar to those previously reported[48]. For nuclei counts and fusion indices, the data distribution was assumed to be normal although this was not formally tested.

Reporting Summary. Further information on research design is available in the Nature Research Reporting Summary linked to this article.

Data availability

RNA-seq data has been deposited to the GEO (accession number GSE173199). Source data are provided with this paper. Further data supporting the findings of this study are available from the authors upon request.

Code availability

Analysis code is available from the authors upon request.

Received: 7 May 2021; Accepted: 1 November 2021;
Published online: 13 January 2022

References

1. Parodi, A. et al. The potential of future foods for sustainable and healthy diets. *Nat. Sustain.* **1**, 782–789 (2018).
2. Post, M. J. et al. Scientific, sustainability and regulatory challenges of cultured meat. *Nat. Food* **1**, 403–415 (2020).
3. Bischoff, R. Regeneration of single skeletal muscle fibers in vitro. *Anat. Rec.* **182**, 215–235 (1975).
4. Collins, C. A. et al. Stem cell function, self-renewal, and behavioral heterogeneity of cells from the adult muscle satellite cell niche. *Cell* **122**, 289–301 (2005).
5. Vandenburgh, H. et al. Tissue-engineered skeletal muscle organoids for reversible gene therapy. *Hum. Gene Ther.* **7**, 2195–2200 (1996).
6. Ben-Arye, T. et al. Textured soy protein scaffolds enable the generation of three-dimensional bovine skeletal muscle tissue for cell-based meat. *Nat. Food* **1**, 210–220 (2020).
7. Pirkmajer, S. & Chibalin, A. V. Serum starvation: caveat emptor. *Am. J. Physiol. Cell Physiol.* **301**, C272–C279 (2011).
8. Das, M. et al. Developing a novel serum-free cell culture model of skeletal muscle differentiation by systematically studying the role of different growth factors in myotube formation. *In Vitro Cell. Dev. Biol. Anim.* **45**, 378–387 (2009).
9. Guo, X. et al. In vitro differentiation of functional human skeletal myotubes in a defined system. *Biomater. Sci.* **2**, 131–138 (2014).
10. Chal, J. et al. Differentiation of pluripotent stem cells to muscle fiber to model Duchenne muscular dystrophy. *Nat. Biotechnol.* **33**, 962–969 (2015).
11. Akiyama, T. et al. Efficient differentiation of human pluripotent stem cells into skeletal muscle cells by combining RNA-based MYOD1-expression and POU5F1-silencing. *Sci. Rep.* **8**, 1189 (2018).
12. Chal, J. & Pourquié, O. Making muscle: skeletal myogenesis in vivo and in vitro. *Development* **144**, 2104–2122 (2017).
13. Millay, D. P. et al. Myomaker: a membrane activator of myoblast fusion and muscle formation. *Nature* **499**, 301–305 (2013).
14. Bryson-Richardson, R. J. & Currie, P. D. The genetics of vertebrate myogenesis. *Nat. Rev. Genet.* **9**, 632–646 (2008).
15. Tsumagari, K. et al. Gene expression during normal and FSHD myogenesis. *BMC Med. Genomics* **4**, 67 (2011).
16. He, H. & Liu, X. Characterization of transcriptional complexity during longissimus muscle development in bovines using high-throughput sequencing. *PLoS ONE* **8**, e64356 (2013).
17. Tripathi, A. K. et al. Transcriptomic dissection of myogenic differentiation signature in caprine by RNA-Seq. *Mech. Dev.* **132**, 79–92 (2014).
18. Lee, E. J. et al. Identification of genes differentially expressed in myogenin knock-down bovine muscle satellite cells during differentiation through RNA sequencing analysis. *PLoS ONE* **9**, e92447 (2014).
19. Nishiyama, T., Kii, I. & Kudo, A. Inactivation of Rho/ROCK signaling is crucial for the nuclear accumulation of FKHR and myoblast fusion. *J. Biol. Chem.* **279**, 47311–47319 (2004).
20. Capkovic, K. L., Stevenson, S., Johnson, M. C., Thelen, J. J. & Cornelison, D. Neural cell adhesion molecule (NCAM) marks adult myogenic cells committed to differentiation. *Exp. Cell. Res.* **314**, 1553–1565 (2008).
21. Tang, Z. et al. Molecular cloning of caveolin-3, a novel member of the caveolin gene family expressed predominantly in muscle. *J. Biol. Chem.* **271**, 2255–2261 (1996).
22. Seale, P. et al. Pax7 is required for the specification of myogenic satellite cells. *Cell* **102**, 777–786 (2000).
23. Weiss, A. & Leinwand, L. A. The mammalian myosin heavy chain gene family. *Annu. Rev. Cell Dev. Biol.* **12**, 417–439 (1996).
24. Pardee, A. B. A restriction point for control of normal animal cell proliferation. *Proc. Natl Acad. Sci. USA* **71**, 1286–1290 (1974).
25. He, K. et al. A transcriptomic study of myogenic differentiation under the overexpression of PPARγ by RNA-Seq. *Sci. Rep.* **7**, 15308 (2017).
26. Massoner, P., Ladurner-Rennau, M., Eder, I. E. & Klocker, H. Insulin-like growth factors and insulin control a multifunctional signalling network of significant importance in cancer. *Br. J. Cancer* **103**, 1479–1484 (2010).
27. Chen, G. et al. Chemically defined conditions for human iPSC derivation and culture. *Nat. Methods* **8**, 424–429 (2011).
28. Breton, C. et al. Presence of functional oxytocin receptors in cultured human myoblasts. *J. Clin. Endocrinol. Metab.* **87**, 1415–1418 (2002).
29. Nikolić, N. et al. Electrical pulse stimulation of cultured skeletal muscle cells as a model for in vitro exercise—possibilities and limitations. *Acta Physiol.* **220**, 310–331 (2017).
30. Gawlitta, D., Boonen, K. J. M., Oomens, C. W. J., Baaijens, F. P. T. & Bouten, C. V. C. The influence of serum-free culture conditions on skeletal muscle differentiation in a tissue-engineered model. *Tissue Eng. A* **14**, 161–171 (2008).
31. Lawson, M. A. & Purslow, P. P. Differentiation of myoblasts in serum-free media: effects of modified media are cell line-specific. *Cells Tissues Organs* **167**, 130–137 (2000).
32. Shoji, E., Woltjen, K. & Sakurai, H. Directed myogenic differentiation of human induced pluripotent stem cells. *Methods Mol. Biol. Clifton NJ* **1353**, 89–99 (2016).
33. Tong, H. L. et al. Transcriptional profiling of bovine muscle-derived satellite cells during differentiation in vitro by high throughput RNA sequencing. *Cell. Mol. Biol. Lett.* **20**, 351–373 (2015).
34. Brunetti, A., Maddux, B. A., Wong, K. Y. & Goldfine, I. D. Muscle cell differentiation is associated with increased insulin receptor biosynthesis and messenger RNA levels. *J. Clin. Invest.* **83**, 192–198 (1989).
35. Ozawa, E. Transferrin as a muscle trophic factor. *Rev. Physiol., Biochem. Pharmacol.* **113**, 89–141 (1989).

36. Cox, R. D., Garner, I. & Buckingham, M. E. Transcriptional regulation of actin and myosin genes during differentiation of a mouse muscle cell line. *Differ. Res. Biol. Divers.* **43**, 183–191 (1990).
37. Hansen, L. H., Abrahamsen, N. & Nishimura, E. Glucagon receptor mRNA distribution in rat tissues. *Peptides* **16**, 1163–1166 (1995).
38. Uhlén, M. et al. Proteomics. Tissue-based map of the human proteome. *Science* **347**, 1260419 (2015).
39. Cencetti, F. et al. Lysophosphatidic acid stimulates cell migration of satellite cells. A role for the sphingosine kinase/sphingosine 1-phosphate axis. *FEBS J.* **281**, 4467–4478 (2014).
40. Yoshida, S., Fujisawa-Sehara, A., Taki, T., Arai, K. & Nabeshima, Y. Lysophosphatidic acid and bFGF control different modes in proliferating myoblasts. *J. Cell Biol.* **132**, 181–193 (1996).
41. Zhang, Z. et al. Oxytocin is involved in steroid hormone-stimulated bovine satellite cell proliferation and differentiation in vitro. *Domest. Anim. Endocrinol.* **66**, 1–13 (2019).
42. Denes, L. T. et al. Culturing C2C12 myotubes on micromolded gelatin hydrogels accelerates myotube maturation. *Skelet. Muscle* **9**, 17 (2019).
43. Stephens, N. et al. Bringing cultured meat to market: technical, socio-political, and regulatory challenges in cellular agriculture. *Trends Food Sci. Technol.* **78**, 155–166 (2018).
44. Furuhashi, M. et al. Formation of contractile 3D bovine muscle tissue for construction of millimetre-thick cultured steak. *NPJ Sci. Food* **5**, 6 (2021).
45. Costantini, M. et al. Microfluidic-enhanced 3D bioprinting of aligned myoblast-laden hydrogels leads to functionally organized myofibers in vitro and in vivo. *Biomaterials* **131**, 98–110 (2017).
46. Lk, L. et al. A pilot study on pain and the upregulation of myoglobin through low-frequency and high-amplitude electrical stimulation-induced muscle contraction. *J. Phys. Ther. Sci.* **26**, 985–988 (2014).
47. Melzener, L., Verzijden, K., Buijs, A., Post, M. & Flack, J. Cultured beef: from small biopsy to substantial quantity. *J. Sci. Food Agric.* **101**, 7–14 (2020).
48. Ding, S. et al. Maintaining bovine satellite cells stemness through p38 pathway. *Sci. Rep.* **8**, 10808 (2018).
49. Liao, Y., Smyth, G. K. & Shi, W. featureCounts: an efficient general purpose program for assigning sequence reads to genomic features. *Bioinformatics* **30**, 923–930 (2014).
50. Yates, A. D. et al. Ensembl 2020. *Nucleic Acids Res.* **48**, D682–D688 (2020).
51. Anders, S. & Huber, W. Differential expression analysis for sequence count data. *Genome Biol.* **11**, R106 (2010).
52. Ritchie, M. E. et al. limma powers differential expression analyses for RNA-sequencing and microarray studies. *Nucleic Acids Res.* **43**, e47 (2015).
53. The Gene Ontology Consortium. The Gene Ontology Resource: 20 years and still GOing strong. *Nucleic Acids Res.* **47**, D330–D338 (2019).
54. Zhang, X. et al. Proteome-wide identification of ubiquitin interactions using UbIA-MS. *Nat. Protoc.* **13**, 530–550 (2018).

Acknowledgements

We thank K. Derks and D. Tserpelis (Genome Services Maastricht UMC+) for their support in the acquisition and analysis of RNA-seq data, R. Mohren (Imaging Mass Spectrometry, M4I, Maastricht University) for proteomics data, and H. Duimel and C. López Iglesia (Microscopy CORE Lab, M4I, Maastricht University) for SEM. We also thank J. Melke and D. Remmers (Mosa Meat BV) for their assistance with confocal microscopy.

Author contributions

T.M., I.K., C.F., E.O., A.D. and J.E.F. performed experiments and analysis. A.D., H.C., M.J.P. and J.E.F. supervised the study. T.M., M.J.P. and J.E.F. wrote the manuscript with input from all authors.

Competing interests

T.M., I.K., C.F., E.O., A.D., H.C. and J.E.F. are employees of Mosa Meat BV. M.J.P. is co-founder and stakeholder of Mosa Meat BV. The study was funded by Mosa Meat BV. Mosa Meat BV has patents pending on serum-free proliferation medium (PCT/P125933PC00) and serum-free differentiation medium (JBB/P126144NL00). All authors declare no other competing interests.

Additional information

Extended data are available for this paper at https://doi.org/10.1038/s43016-021-00419-1.

Supplementary information The online version contains supplementary material available at https://doi.org/10.1038/s43016-021-00419-1.

Correspondence and requests for materials should be addressed to Joshua E. Flack.

Peer review information *Nature Food* thanks Deepak Choudhury, Laura Domigan and Min Du for their contribution to the peer review of this work.

Reprints and permissions information is available at www.nature.com/reprints.

Publisher's note Springer Nature remains neutral with regard to jurisdictional claims in published maps and institutional affiliations.

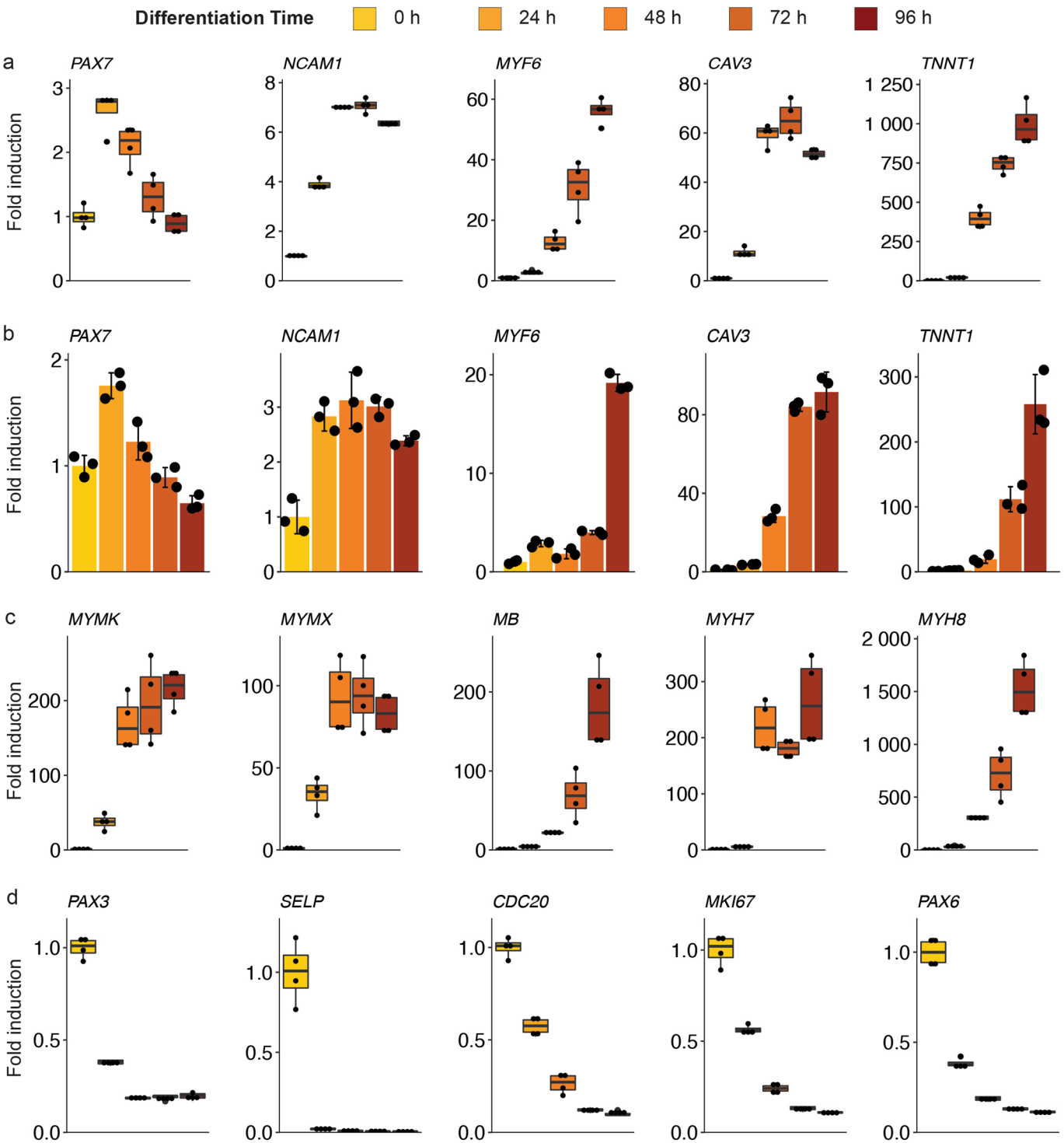

Extended Data Fig. 1 | Gene expression during myogenic differentiation induced by serum starvation (related to Fig. 1). a, RNA-seq-derived median fold changes of selected muscle-related genes during serum starvation compared to 0 h. **b**, Mean fold changes of genes shown in a), determined via RT-qPCR; error bars indicate SD, $n = 3$. **c**, Median fold changes of selected strongly upregulated myogenic genes compared to 0 h, determined via RNA-seq. **d**, Median fold changes of selected downregulated genes compared to 0 h, determined via RNA-seq; boxes indicate IQR, whiskers show 1.5 × IQR.

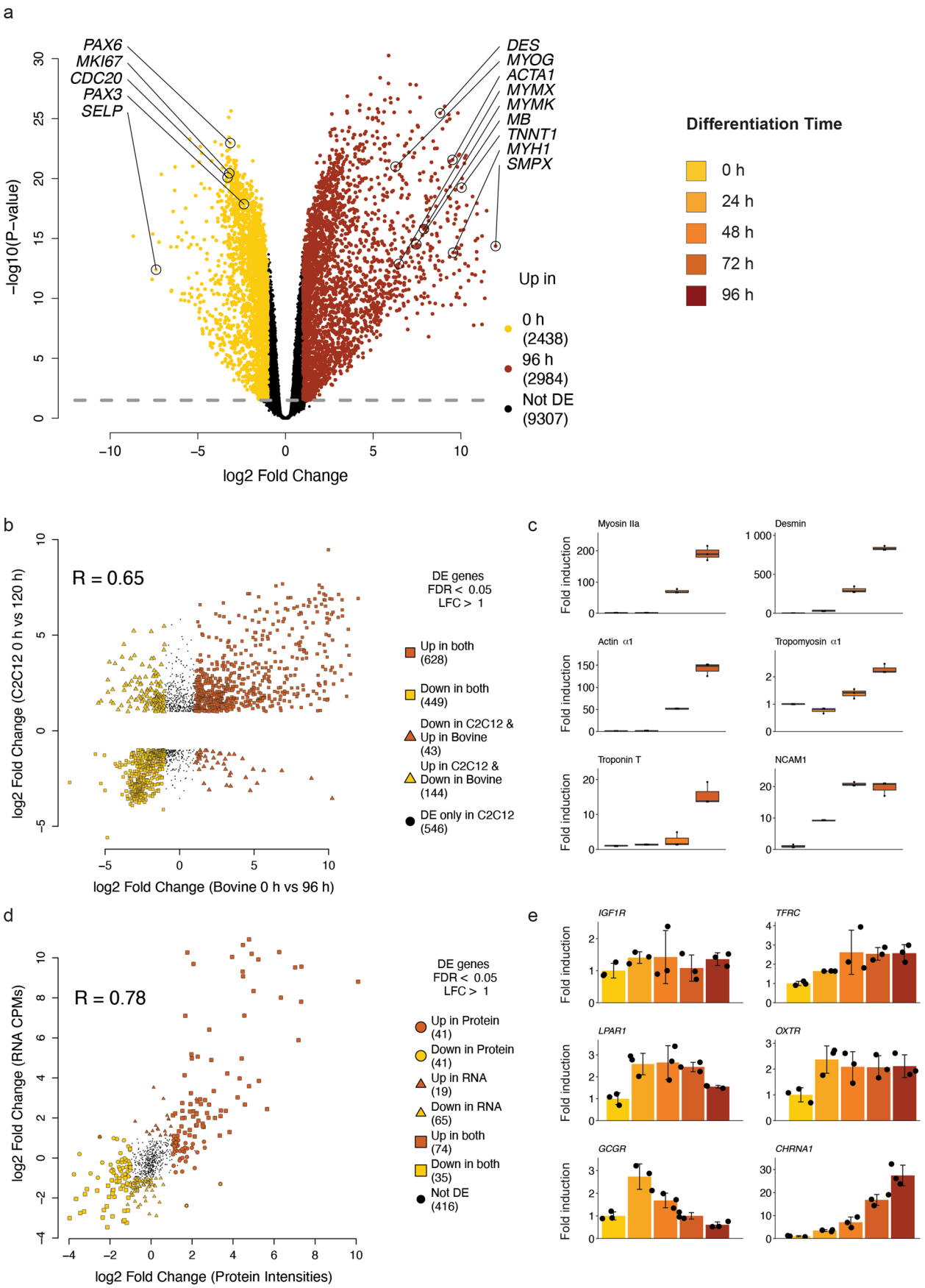

Extended Data Fig. 2 | See next page for caption.

Extended Data Fig. 2 | Transcriptomic and proteomic characterisation of serum starvation (related to Fig. 2). a, Volcano plot showing differentially expressed genes between 0 h (yellow) and 96 h (red) of serum starvation. Selected differentially expressed muscle, stem cell or cell cycle-related genes are indicated. **b**, Scatter plot showing correlation of log2-fold changes of overlapping genes from bovine (x-axis) with C2C12 (y-axis) with indicated Pearson correlation coefficient (R). Colours indicate upregulation (red) or downregulation (yellow) in bovine gene expression, shapes indicate whether differentially expressed genes are simultaneously up/downregulated in both species (squares) or significantly up/downregulated in one species while inversely regulated in the other (triangles). **c**, Median fold changes of muscle-related protein levels from 0 h to 72 h post serum starvation, normalised against 0 h; boxes indicate IQR, whiskers show 1.5 × IQR. **d**, Scatter plot showing the Pearson correlation of log2-fold changes of genes from RNA-seq (y-axis) and corresponding proteins from mass spectrometry (x-axis) upon serum starvation with indicated correlation coefficient (R). Colours indicate upregulation (red) or downregulation (yellow) while shapes indicate significantly regulated proteins (points), genes (triangles), or both (squares). **e**, Mean fold gene expression changes of differentially regulated surface receptors, determined by RT–qPCR; error bars indicate SD, $n = 3$.

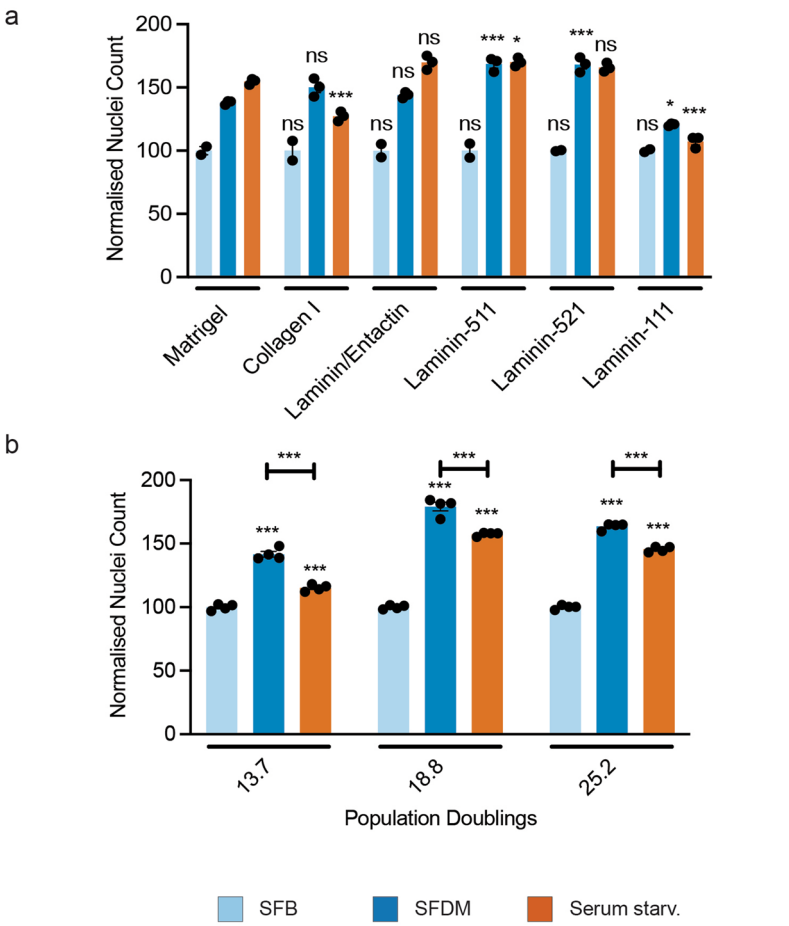

Extended Data Fig. 3 | See next page for caption.

Extended Data Fig. 3 | Serum-free differentiation and serum starvation are similar with respect to cell age and coating (related to Fig. 4). a, Normalised nuclei counts of SCs differentiating on indicated coatings after 72 h in SFB, SFDM and serum starvation as percentage against SFB; statistical significance is indicated for each media against respective Matrigel control, error bars indicate SD, $n = 3$. **b**, Normalised nuclei counts of SCs after 72 h of SFB, SFDM or serum starvation at early (left), medium (centre), and late (right) passages with indicated PDs, as percentage of low PDs in SFB; asterisks directly above bars indicate statistical significance against SFB; error bars indicate SD, $n = 4$. **c**, Representative fluorescence images of differentiating SCs at early (top), medium (middle) or late (bottom row) passages after 72 h in SFB (left), SFDM (centre) or serum starvation (right), corresponding to Fig. 4e, Extended Data Fig. 3b; green, desmin; blue, Hoechst. Scale bar, 500 µm. *$P < 0.05$, **$P < 0.005$, ***$P < 0.001$.

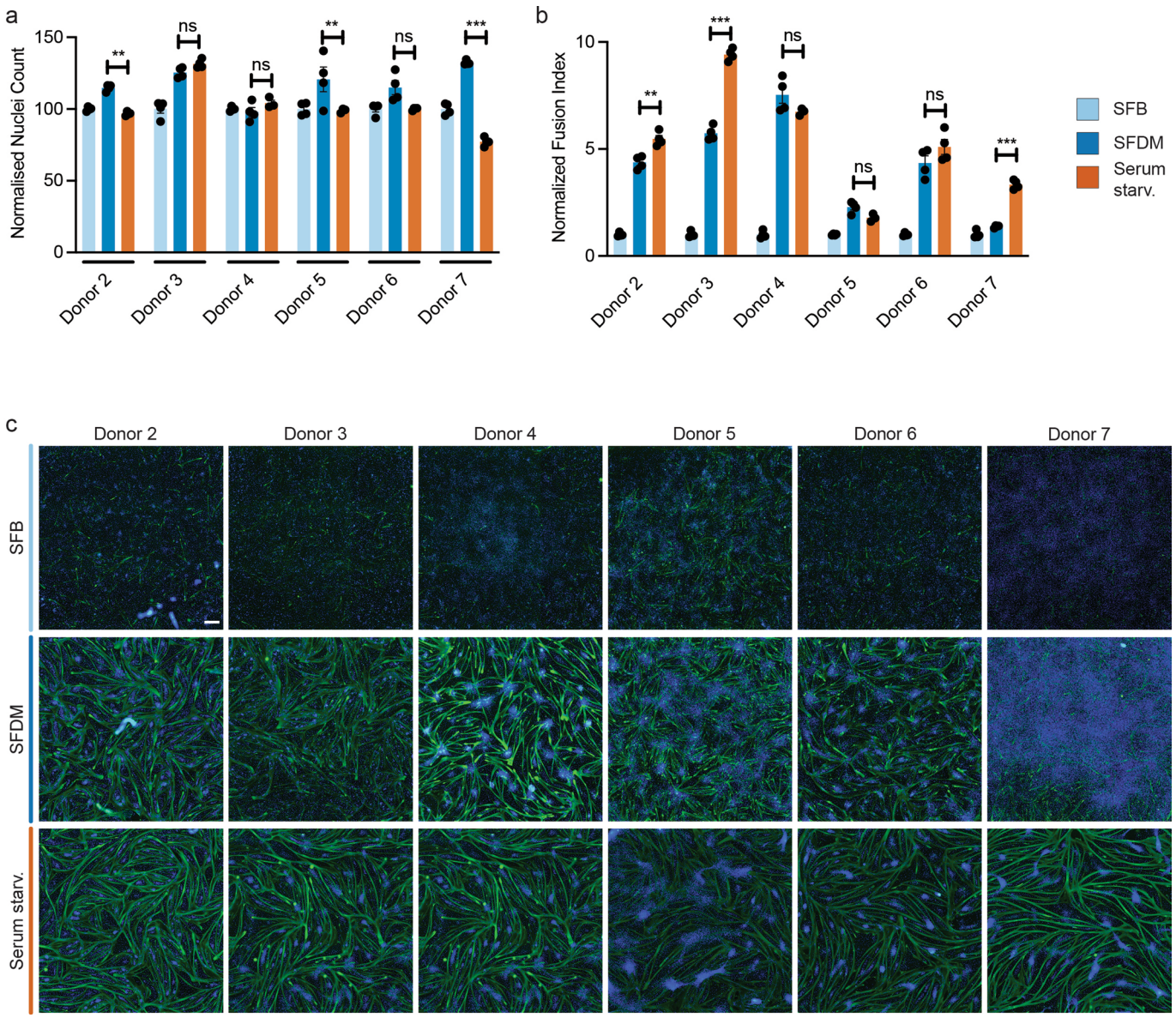

Extended Data Fig. 4 | Extent of serum-free differentiation varies between donor animals (related to Fig. 4). a, Normalised nuclei counts of SCs from different donor animals after 72 h of myogenic differentiation as percentage of SFB with statistical significance indicated between SFDM and serum starvation respectively for each donor; error bars indicate SD, $n = 4$. **b**, Mean fusion indices of SCs from different donor animals after 72 h of serum-free or serum starvation induced differentiation, normalised against respective SFB condition. Statistical significance is indicated between SFDM and serum starvation respectively for each donor; error bars indicate SD, $n = 4$. **c**, Representative fluorescence images of myogenic differentiation of SCs from different donor animals after 72 h in SFB (top), SFDM (middle) and serum starvation (bottom row); green, desmin; blue, Hoechst. Scale bar, 500 µm. *$P < 0.05$, **$P < 0.005$, ***$P < 0.001$.

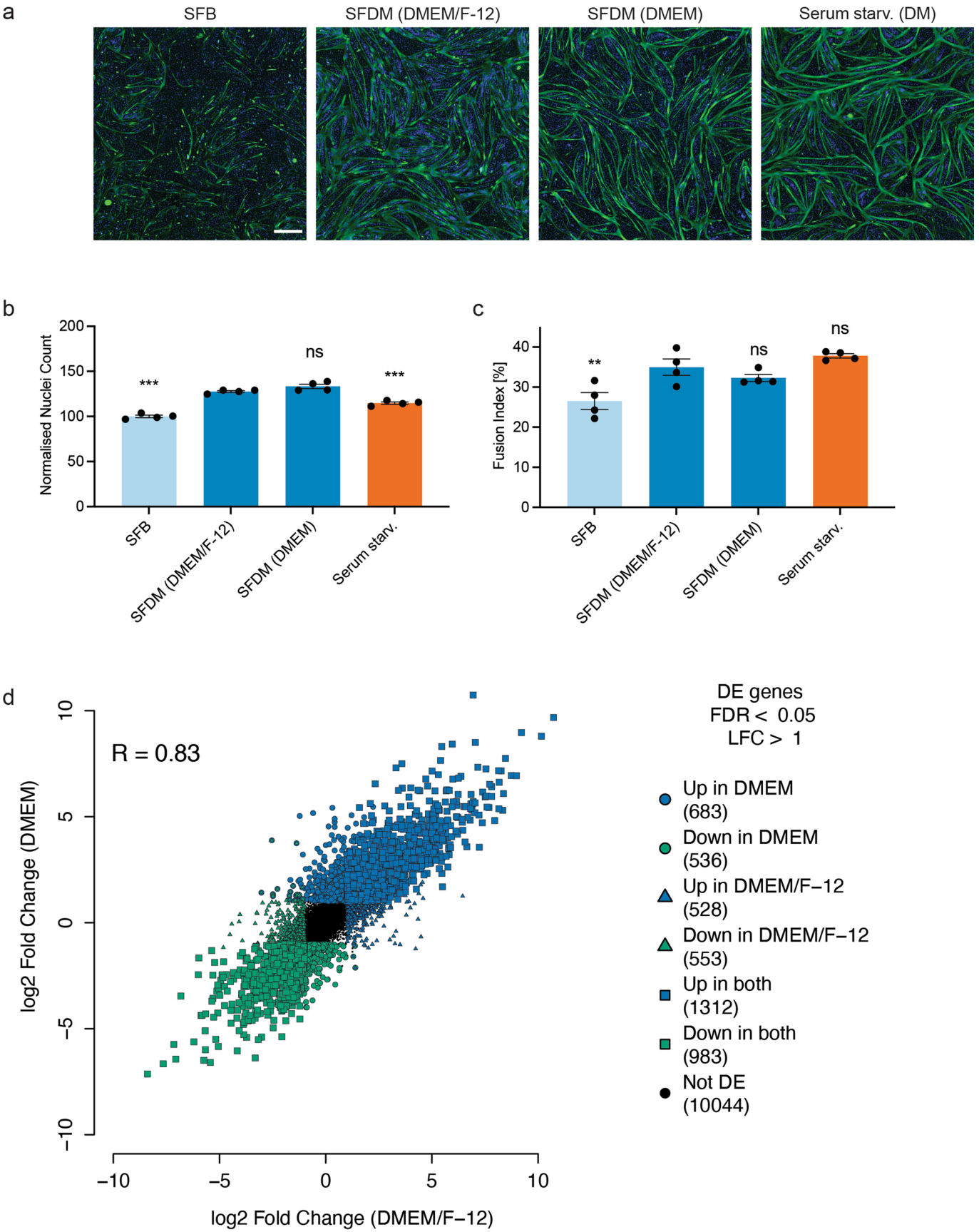

Extended Data Fig. 5 | See next page for caption.

Extended Data Fig. 5 | 2D serum-free differentiation can be achieved with different basal media (related to Fig. 6). a, Representative fluorescence images of SCs after 72 h in SFB, SFDM with DMEM/F-12 and DMEM base, and upon serum starvation; green, desmin; blue, Hoechst. Scale bar, 500 μM. **b**, Normalised nuclei counts from a) as percentage of SFB with statistical significance indicated against SFDM (DMEM/F-12); error bars indicate SD, $n = 4$. **c**, Mean fusion indices derived from a) with statistical significance performed against SFDM (DMEM/F-12); error bars indicate SD, $n = 4$. **d**, Scatter plot indicating correlation of log2-fold changes between SFGM and DMEM/F-12-based SFDM (x-axis) against log2-fold changes between SFGM and DMEM-based SFDM (y-axis) with Pearson correlation coefficient indicated. *$P < 0.05$, **$P < 0.005$, ***$P < 0.001$.

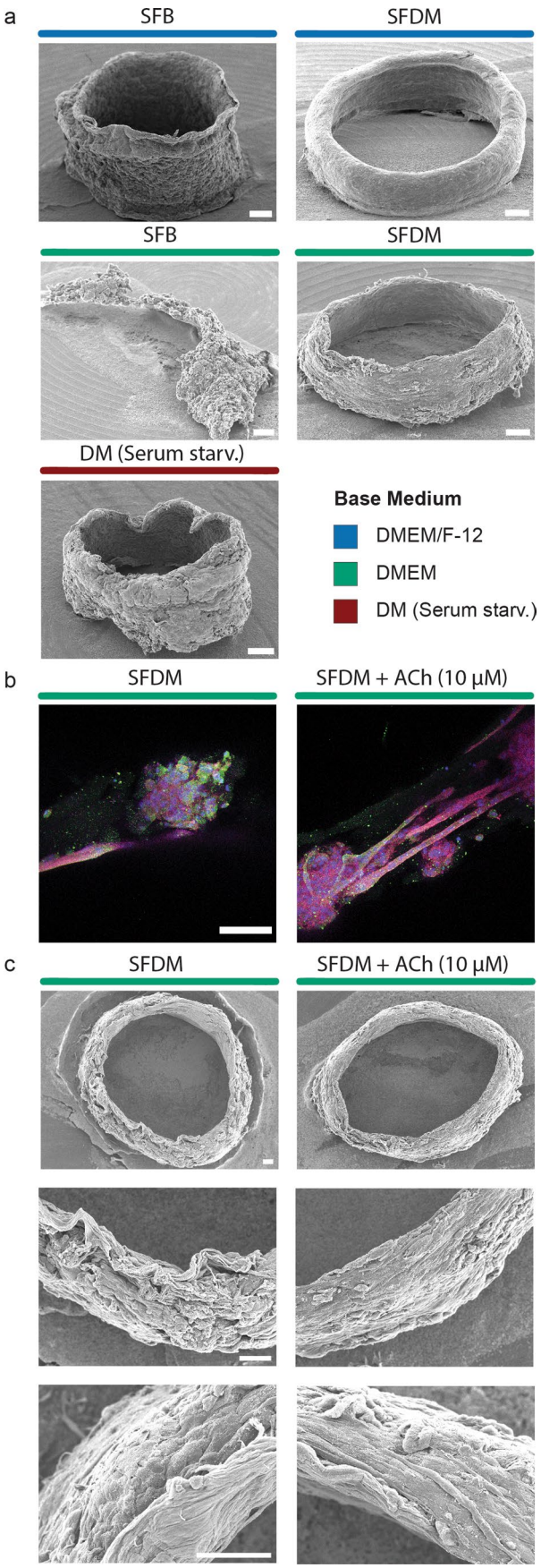

Extended Data Fig. 6 | See next page for caption.

Extended Data Fig. 6 | Acetylcholine supplementation improves myogenic fusion in bioartificial muscles (related to Fig. 6). a, Ultrastructure of BAMs after 192 h in SFB or SFDM (with DMEM/F-12 or DMEM basal media) or serum starvation. Scale bar, 100 µm. **b**, Representative fluorescence images of BAMs after 192 h in DMEM-based SFDM without (left) and with (right) 10 µM acetylcholine (ACh); pink, desmin; red, α-actin; green, myosinHC; blue, Hoechst. Scale bars, 100 µm. **c**, Ultrastructure (top), wide (middle) and close-up (bottom) scanning electron microscopy images of BAMs after 192 h in DMEM-based SFDM with (right) and without (left) 10 µM acetylcholine. Scale bars, 100 µm.

Extended Data Table 1 | Media Formulations

Component	Concentration
Growth medium (GM)	
Ham's F-10 Nutrient Mix (31550-023, Gibco) +	
Fetal Bovine Serum (FBS)	20%
FGF2	5 ng ml^{-1}
Penicillin/Streptomycin/Amphotericin (PSA; 17-745E, Lonza)	1%
Differentiation medium (DM)	
DMEM (22320-022, Gibco) +	
FBS	2%
PSA	1%
Serum-free growth medium (SFGM)	
DMEM/F-12 (21331-020, Gibco) +	
Chemically-defined FBS replacement	1%
PSA	1%
Serum-free base medium (SFB)	
DMEM/F-12 (or DMEM where indicated) +	
EGF1	10 ng ml^{-1}
Human Serum Albumin	0.5 mg ml^{-1}
L-ascorbic acid 2-phosphate (Vitamin C)	40 µM
MEM Amino Acids Solution (11130-051, ThermoFisher)	0.5%
$NaHCO_3$	6.5 mM
PSA	1%
Sodium Selenite	80 nM
Serum-free differentiation medium (SFDM)	
SFB +	
Insulin	1.8 µM
LPA	1 µM
Transferrin	135 nM
ACh (for BAM fabrication after 96 h)	10 µM

Extended Data Table 2 | RT-qPCR primers

Gene		Primer Sequence
B2M	Fwd:	5'-TGGAGGTGCTGGCATCTTAG
	Rev:	5'-ATGCAGAAGACACCCAGATGTT
CAV3	Fwd:	5'-GATCGATCTGGTGAACCGGG
	Rev:	5'-TGTAGCTCACCTTCCACACG
CHRNA1	Fwd:	5'-ACTTCATGGAGAGCGGAGAA
	Rev:	5'-AACACTAGGCCGGTCAAGAA
DES	Fwd:	5'-GGAAGCCGAGGAATGGTACA
	Rev:	5'-TCGATCTCGCAGGTGTAGGA
GCGR	Fwd:	5'-CGGAGGCTAGAGTGTGGAAG
	Rev:	5'-GAATGTGGACACGCTGACAC
IGF1R	Fwd:	5'-CCTCCACATCCTGCTCATTT
	Rev:	5'-GATGACCAGGGCGTAGTTGT
LPAR1	Fwd:	5'-CCGCAGTGCTTCTACAATGA
	Rev:	5'-GCCAGATTCGCCATAAGGTA
MYOD1	Fwd:	5'-CGACGGCATGATGGACTACA
	Rev:	5'-GTAAGTGCGGTCGTAGCAGT
MYF5	Fwd:	5'-TCTATCTCTCTGCTGTCCAGGC
	Rev:	5'-AACTCGTCCCCGAACTCAC
MYF6	Fwd:	5'-GCGAGAGGCGGCGGCTCAAGAAAATCAACG
	Rev:	5'-TGGAATGATCCGAAACACTTGGCCACTG
NCAM1	Fwd:	5'-CCGAGAAGGGTCCCGTAGA
	Rev:	5'-ATTTGTGTGGCATCGTTGGG
OXTR	Fwd:	5'-TCCACGCTGTGACTGATAGG
	Rev:	5'-GCTTGGTTTGATGGTGGAGT
PAX7	Fwd:	5'-CTCCCTCTGAAGCGTAAGCA
	Rev:	5'-GGGTAGTGGGTCCTCTCGAA
RPL19	Fwd:	5'-TCGAATGCCCGAGAAGGTAAC
	Rev:	5'-CTGTGATACATGTGGCGGTC
TFRC	Fwd:	5'-GGCTCTGGCTCTCACACTCT
	Rev:	5'-TTCGTTGTCAATGTCCCAAA
TNNT1	Fwd:	5'-CCTCTGATCCCGCCAAAGAT
	Rev:	5'-GGTCCTTTTCCATGCGCTTC
TPM1	Fwd:	5'-GAGTTGAAAACTGTGACGAACAAC
	Rev:	5'-ACCTCTCCGCAAACTCAGC

nature research

Corresponding author(s): Joshua E Flack

Last updated by author(s): 22.10.21

Reporting Summary

Nature Research wishes to improve the reproducibility of the work that we publish. This form provides structure for consistency and transparency in reporting. For further information on Nature Research policies, see our Editorial Policies and the Editorial Policy Checklist.

Statistics

For all statistical analyses, confirm that the following items are present in the figure legend, table legend, main text, or Methods section.

n/a	Confirmed	
☐	☒	The exact sample size (*n*) for each experimental group/condition, given as a discrete number and unit of measurement
☐	☒	A statement on whether measurements were taken from distinct samples or whether the same sample was measured repeatedly
☐	☒	The statistical test(s) used AND whether they are one- or two-sided *Only common tests should be described solely by name; describe more complex techniques in the Methods section.*
☐	☒	A description of all covariates tested
☐	☒	A description of any assumptions or corrections, such as tests of normality and adjustment for multiple comparisons
☐	☒	A full description of the statistical parameters including central tendency (e.g. means) or other basic estimates (e.g. regression coefficient) AND variation (e.g. standard deviation) or associated estimates of uncertainty (e.g. confidence intervals)
☐	☒	For null hypothesis testing, the test statistic (e.g. *F*, *t*, *r*) with confidence intervals, effect sizes, degrees of freedom and *P* value noted *Give P values as exact values whenever suitable.*
☐	☒	For Bayesian analysis, information on the choice of priors and Markov chain Monte Carlo settings
☐	☒	For hierarchical and complex designs, identification of the appropriate level for tests and full reporting of outcomes
☐	☒	Estimates of effect sizes (e.g. Cohen's *d*, Pearson's *r*), indicating how they were calculated

Our web collection on statistics for biologists contains articles on many of the points above.

Software and code

Policy information about availability of computer code

Data collection	RNA sequencing STAR aligner 2.769 was used to align single-end reads from BAM files to the reference genome bosTau9 (ARS UCD1.2.98). For protein identification and quantification, DDA spectra were analyzed with MaxQuant (Max Planck Institute) to generate LFQ intensities.
Data analysis	Subsequent analyses of the RNA-sequencing data and the proteomic data were performed using R 4.0.3.

For manuscripts utilizing custom algorithms or software that are central to the research but not yet described in published literature, software must be made available to editors and reviewers. We strongly encourage code deposition in a community repository (e.g. GitHub). See the Nature Research guidelines for submitting code & software for further information.

Data

Policy information about availability of data

All manuscripts must include a data availability statement. This statement should provide the following information, where applicable:

- Accession codes, unique identifiers, or web links for publicly available datasets
- A list of figures that have associated raw data
- A description of any restrictions on data availability

RNA-seq data are available under GEO accession number GSE173199 (and can be accessed at https://www.ncbi.nlm.nih.gov/geo/query/acc.cgi?acc=GSE173199). Proteomic data is available as Supplementary Table 2.

Field-specific reporting

Please select the one below that is the best fit for your research. If you are not sure, read the appropriate sections before making your selection.

☒ Life sciences ☐ Behavioural & social sciences ☐ Ecological, evolutionary & environmental sciences

For a reference copy of the document with all sections, see nature.com/documents/nr-reporting-summary-flat.pdf

Life sciences study design

All studies must disclose on these points even when the disclosure is negative.

Sample size	Triplicates or quadruplicate samples were performed for all experiments. No sample-size calculation was performed. These sample sizes were deemed sufficient for robust P-value calculations.
Data exclusions	No data were excluded from the analyses.
Replication	All key results were replicated in at least two separate experiments.
Randomization	Randomization was not applicable to this study (since cells from all donor animals were tested in all conditions).
Blinding	Data collectors were blinded to group allocation of samples by numbering the conditions during data acquisition.

Reporting for specific materials, systems and methods

We require information from authors about some types of materials, experimental systems and methods used in many studies. Here, indicate whether each material, system or method listed is relevant to your study. If you are not sure if a list item applies to your research, read the appropriate section before selecting a response.

Materials & experimental systems

n/a	Involved in the study
☐	☒ Antibodies
☒	☐ Eukaryotic cell lines
☒	☐ Palaeontology and archaeology
☒	☐ Animals and other organisms
☒	☐ Human research participants
☒	☐ Clinical data
☒	☐ Dual use research of concern

Methods

n/a	Involved in the study
☒	☐ ChIP-seq
☒	☐ Flow cytometry
☒	☐ MRI-based neuroimaging

Antibodies

Antibodies used	anti-desmin (D1033, Sigma Aldrich), anti-myogenin (sc-52903, Santa Cruz Biotechnology), anti-tropomyosin-alpha1 (ab133292, Abcam), anti-myosin heavy chain beta (myosinHC) (M8421, Sigma Aldrich), anti-alpha-actin (ab97373, Abcam), anti-alpha-tubulin (ab4074, Abcam), anti-mouse-HRP (ab6721, Abcam), anti-rabbit-HRP (P0447, Dako), anti-rabbit-Alexa488 (A21206,Thermo Fisher Scientific), anti-mouse-Alexa633 (A21050, Thermo Fisher Scientific), anti-NCAM1-PE-Cy7 (335826, BD Biosciences), anti-CD29-APC (B247653, BioLegend), anti-CD31-FITC (MCA1097F, Bio-Rad), anti-CD45-FITC (MCA2220F, Bio-Rad)
Validation	Antibodies 335826, B247653, MCA1097F and MCA2220F were validated in Ding et al., 2018 (PMID: 30018348). For D1033, M8421, ab97373, and ab4074, cross-reactivity with bovine was confirmed by manufacturer. For antibodies previous unvalidated in bovine samples (sc-52903, ab133292), a bovine muscle positive control sample was performed.